Chemical Engineering Journal 366 (2019) 339–357

Contents lists available at ScienceDirect

Chemical Engineering Journal

journal homepage: www.elsevier.com/locate/cej

Review

Application of silver phosphate-based photocatalysts: Barriers and solutions

Xiaopei Li[a,b,1], Piao Xu[a,b,1], Ming Chen[a,b,1], Guangming Zeng[a,b,*], Dongbo Wang[a,b,*], Fei Chen[a,b], Wangwang Tang[a,b], Changya Chen[a,b], Chen Zhang[a,b], Xiaofei Tan[a,b]

[a] College of Environmental Science and Engineering, Hunan University, Changsha 410082, China
[b] Key Laboratory of Environmental Biology and Pollution Control (Hunan University), Ministry of Education, Changsha 410082, China

HIGHLIGHTS

- Fundamental mechanism for the excellent photocatalytic performance of Ag_3PO_4.
- Synthesis methods for Ag_3PO_4 with high photocatalytic performance.
- Barriers and solutions for the practical application of Ag_3PO_4.

GRAPHICAL ABSTRACT

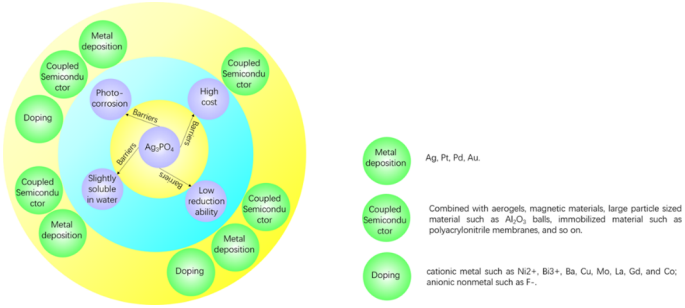

ARTICLE INFO

Keywords:
Synthesis method
Barrier
Metal deposition
Hybrid composite
Doping
Photoreactor

ABSTRACT

Semiconductor photocatalysis is an extremely promising technology to deal with the far-reaching issues we need to face, such as the shortage of renewable-energy resources and the increasingly serious worldwide environmental problems. Ag_3PO_4 is an excellent visible-light-driven photocatalyst, showing an extraordinary photoactivity for oxygen evolution in water splitting and degradation of pollutant in aqueous solution. However, due to the uncontrollable photocorrosion phenomenon, the Ag_3PO_4-based photocatalysis is still at laboratory scale. To remove the obstacles for practical application and to further improve its photocatalytic performance, this review summarized the achievements that have been made in this field. We began with an effort to introduce the reasons for Ag_3PO_4 exhibiting excellent photocatalytic performance. Subsequently, the different synthesis methods of Ag_3PO_4 were discussed. Finally, we outlined the barriers that hindered the practical application of Ag_3PO_4 and proposed the ways to remove these barriers. This review also underlined the crucial problems that should be addressed prior to practical applications.

1. Introduction

Facing the increasingly serious environmental issues, many methods have been developed to solve these problems, such as adsorption, bioremediation, and advanced oxidation processes [1–17]. Among them, photocatalysis is a promising method that has attracted more and more attention, because it represents an easy way to take advantage of solar energy and it could be abundantly available everywhere in the world [18–24]. It is undoubted that the semiconductor photocatalysis is an extremely promising technology to handle the far-reaching issues faced by us, e.g., the growing renewable-energy shortage crisis and environmental problems [23]. The photocatalytic industry has ushered

* Corresponding authors at: College of Environmental Science and Engineering, Hunan University, Changsha 410082, China.
E-mail addresses: zgming@hnu.edu.cn (G. Zeng), dongbowang@hnu.edu.cn (D. Wang).
[1] These authors contributed equally to this work.

https://doi.org/10.1016/j.cej.2019.02.083
Received 16 November 2018; Received in revised form 13 January 2019; Accepted 12 February 2019
Available online 13 February 2019
1385-8947/

in an era of flourishing ever since Fujishima and Honda [25] reported that TiO_2 could be used as an electrode under ultra-violet radiation for photoelectrochemical water splitting back in 1970s.

Give the credit to the properties of TiO_2 (e.g., electronic structure, chemical stability, and low cost), it is unquestionable that TiO_2 is an extremely promising photocatalyst. However, restrained by its wide band gap energy (E_g = 3.23 eV), TiO_2 is mainly excited under ultra violet irradiation, suggesting that it could only utilize 4% of solar energy at most [26]. To promote the efficiency of solar energy utilization, extending the corresponding region to visible-light is a practicable solution. To achieve this goal, there are generally two ways: One is the combination of TiO_2 with other materials such as non-metal ions (e.g., N, C, and S) [27–29], halogen [30,31], transition metal ions (e.g., Fe, Cr, Mn, and V) [32,33], noble metal ions [34], graphene [35–37], and semiconductor (e.g., CdS-TiO_2 [38], CdSe-TiO_2 [39], Bi_2O_3-TiO_2 [40], WO_3-TiO_2 [41], Cu_2O-TiO_2 [42], and SnO_2-TiO_2 [43]) or doping other elements into the crystal of TiO_2 [44–47]; another is the development of some novel semiconductor photocatalysts such as tungsten-containing photocatalyst [48], bismuth-based photocatalyst [49,50], g-C_3N_4 [51], and Ag_3PO_4 [52]. Among them, Ag_3PO_4 was demonstrated to have a superior performance in the field of oxygen rate and dye degradation. Thus, Ag_3PO_4 has attracted great attention ever since Ye and co-workers [52] discovered its photocatalytic application in 2010.

Ag_3PO_4 is a photocatalyst which can be excited by visible light. Its band gap energy is approximately 2.43 eV [52]. Generally, pure Ag_3PO_4 photocatalyst could absorb solar energy with a wavelength shorter than 530 nm. The valence band of Ag_3PO_4 is approximately +2.9 V vs. normal hydrogen electrode (NHE, pH = 0), suggesting that it possesses strong oxidizing property. Moreover, quantum efficiency of Ag_3PO_4 could reach approximately 90% in water oxidation (while using $AgNO_3$ as scavenger). This is greater than the widely known photocatalysts such as N-doped TiO_2 and $BiVO_4$ [52]. Ag_3PO_4 could serve as an efficient photocatalyst for the treatment of environmental contaminants, such as phenol and phenol derivatives [53–56], humic acid [57], Cr(VI) [58], dyes [15,59,60], endocrine disrupting compounds [61], pharmaceuticals and personal care products [21,62–64]. Despite these benefits, practical application of Ag_3PO_4-based photocatalysis has not been achieved to date, due to several key barriers such as the high cost of raw materials, the slightly soluble in water, and the self-photocorrosion phenomenon [65,66]. Herein, in this review, we aim to offer a systematically summarization and reasonable suggestions about how to remove the obstacles that impede the practical application of Ag_3PO_4 in a full-scale situation.

2. Why does Ag_3PO_4 show excellent photocatalytic performances?

The crystal structure of Ag_3PO_4 is a body-centered cubic (BBC) which is composed of several isolated, regular PO_4 tetrahedral unit cells, with its P-O bonds distance being about 1.539 Å. The space group of Ag_3PO_4 is P4-3n with a lattice parameter of approximately 6.004 Å (inset of Fig. 1). The location of its valence band is much lower than the O_2/H_2O potential (+1.23 V vs. NHE), meaning that it has extraordinary oxidation capability (Fig. 1). Owing to the position of the conduction band of Ag_3PO_4 (+0.45 V vs. NHE, pH = 0), the photogenerated electrons would be more likely to react with oxygen to produce H_2O_2 ($2e^- + 2H^+ + O_2 \rightarrow H_2O_2$) instead of producing $^{\cdot}O_2^-$ or $^{\cdot}HO_2^-$ active oxygen species. In the mean time, photogenerated holes would directly participate in the oxidation reaction (pollutant + $h^+ \rightarrow$ $CO_2 + H_2O$ + other products; $2H_2O + 4h^+ \rightarrow O_2 + 4H^+$) despite of the valence band of Ag_3PO_4 is positive enough to react with H_2O to produce ·OH. Direct hole oxidation is overmatched the traditional free radical oxidation. According to Fu et al. [67], although the potential of holes generated by Bi_2WO_6 is insufficient to form ·OH radicals, Bi_2WO_6 still is able to dechlorine of 4-chlorophenol, to oxidize $CHCl_3$ and CH_3CHO [68], or to split water for oxygen evolution [69]. Ag_3PO_4 has

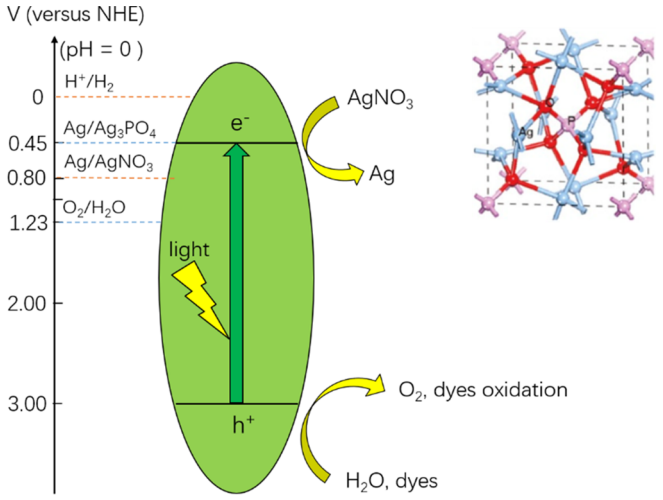

Fig. 1. Schematic diagram of photocatalytic redox process of Ag_3PO_4. Inset: ball and stick configuration of Ag_3PO_4 (the inset is cited from Ref. [71]).

strong oxidation capability and high thermal stability. For instance, Teng et al. [65] announced that Rh B could be thoroughly degraded by Ag_3PO_4 polypods after 36 h under natural indoor weak light irradiation, while only 18% for N-doped TiO_2 after 120 h under the same condition. Zhang et al. [70] declared that Ag_3PO_4 could keep a good structure and thermal stability below 540 °C, and Ag_3PO_4 samples with annealing process (100 and 400 °C) shows better photocatalytic activity to Rh B than that of Ag_3PO_4 samples without sintering. The structure of Ag_3PO_4 still remains even after sintering at 400 °C for 90 min, and only a few thin Ag nanoparticles were detected after 120 min.

Plenty of researchers have demonstrated that Ag_3PO_4 exhibited extremely high photocatalytic capability in both oxygen production by water splitting and photodegradation of organic contaminant. To understand why Ag_3PO_4 shows an outstanding photocatalytic performance, we briefly summarized the articles available, and attributed the outperformed photocatalytic activities of Ag_3PO_4 to the following reasons. First, the constitution and distribution of the conduction band minimum (CBM) of Ag_3PO_4 are useful to the electron transfer [72]. The formation of a rigid tetrahedral unit of PO_4 makes the CBM mainly be constituted by Ag s states in Ag_3PO_4 as well as a fully occupied d state in the valence band maximum (VBM). The CBM of Ag_3PO_4 is well dispersed without the so-called "contaminant" of d states, which decreased the effective mass of electrons of Ag_3PO_4, and favors its transfer (Fig. 2). Besides, Ag_3PO_4 has a very isotropic distribution of CBM, which makes the chance of meeting photoinduced holes decreases compare to the semiconductors with anisotropic distribution. Second, the inductive effect of PO_4^{3-} is favors for the separation of electron-hole pairs [73]. The large electron clouds overlapping of PO_4^{3-} ions makes it more likely to draw holes and reject electrons, which reduced the recombination of photogenerated charge carriers, and enhanced the photocatalytic activity. Third, native defects such as Ag vacancies are favorable for the photocatalytic activity [73]. Ag vacancies are inevitably yield due to the photocorrosion of Ag_3PO_4. It behaves as shallow acceptor (since the outer electron of Ag atoms is easier to escape than that of P atoms) and has a high concentration in Ag_3PO_4. By acting as capture traps for photogenerated holes, it can inhibit the recombination of charge carriers, thus promoting the photocatalytic capability of Ag_3PO_4. In brief, the excellent photocatalytic performance of Ag_3PO_4 could be credited to the separation efficiency of photogenerated electron-hole pairs. Besides, there might be some other reasons for superb photocatalytic capacity of Ag_3PO_4 that have not been identified yet, and further work requires to be carried out in the future.

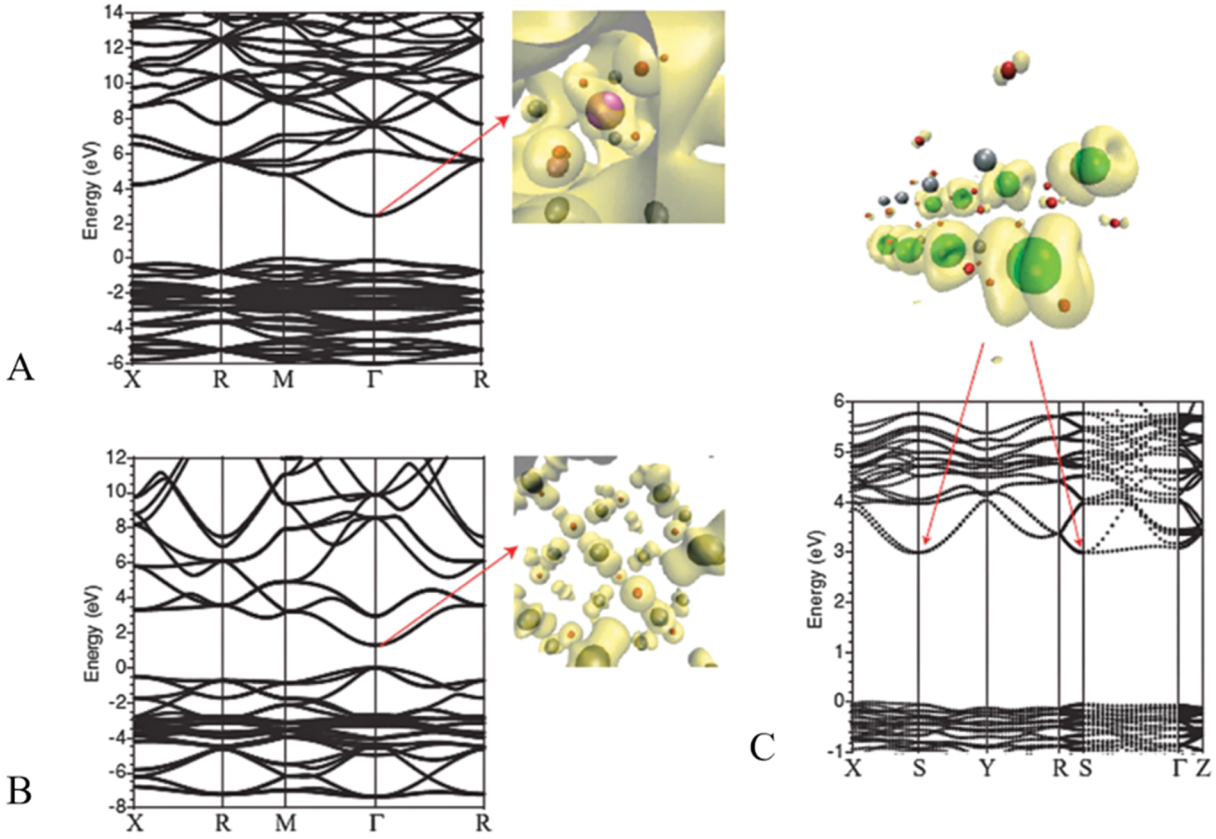

Fig. 2. Band structures and the square of wave function (inset) corresponding to the CBM for (A) Ag_3PO_4, (B) Ag_2O, and (C) $AgNbO_3$ (cited from Ref. [72]).

3. How to synthesize Ag_3PO_4-based photocatalysts?

There are four fundamental steps for a photocatalysis process: the generation of electron-hole pairs, the separation of photoinduced electron-hole pairs, the migration of electron-hole pairs to the surface, and the redox reactions. The migration of electron-hole pairs to the surface process normally would be affected by the particle size, surface state, crystallinity, crystal texture, and so on. For instance, a short transfer distance of charge carriers is undoubtedly beneficial to the decreases of the recombination. On the other hand, the surface of photocatalysts is the place where the photocatalysis process occurs. The synthesis process of photocatalyst is closely related to those influence factors. In recent years, lots of synthesis methods have been proposed to fabricate Ag_3PO_4-based photocatalyst [57,74–81], and we summarized the most commonly used approaches in the following texts (Table 1).

3.1. Ion-exchange method

Ion-exchange method is the mostly used method for the fabrication of Ag_3PO_4. It takes advantage of the different solubility of raw materials such as AgM and NPO_4 (M and N are the ions or ionic group except for Ag^+ and PO_4^{3-}, respectively), to replace M^- or N^{3+} by PO_4^{3-} or Ag^+, thereby forming Ag_3PO_4 particles. The operation condition is simple, and the cost is low. It synthesizes Ag_3PO_4 samples at room temperature without special equipment. The choice of raw material is the key technology in this method. Yu et al. [74] recently synthesized a one-dimensional Ag_3PO_4 hollow microrods with extremely high photocatalytic performance and self-stability through anion exchange method. Ag_2WO_4 was utilized as Ag^+ ion sources instead of $AgNO_3$ or CH_3COOAg. Ag_3PO_4 has lower solubility compared to Ag_2WO_4, and thus Ag_2WO_4 could react with HPO_4^{2-} ions to form Ag_3PO_4 in a thermodynamically favored direction. In this reaction procedure, the released Ag^+ ions are really close to the Ag_2WO_4. The inward HPO_4^{2-} is slower compare to the outward Ag^+, which favors the formation of a hollow interior (Fig. 3). The as-obtained Ag_3PO_4 has perfect and regular 1D structure with 2 μm in diameter and 2 μm in length, which is similar to the Ag_2WO_4 microrods precursor. The Ag_3PO_4 samples as synthesized could thoroughly photodegrade Rh B within 60 s and MO in 60 s, whilst spherical particles needed 14 min and 28 min, respectively. In addition, the 5-cycle run test demonstrated that this structure could serve as a viable way to enhance the stability of Ag_3PO_4.

3.2. Precipitation method

The precipitation method is also frequently used for Ag_3PO_4 fabrication. Keisuke et al. [57] demonstrated that the samples fabricated by precipitation methods possessed higher photooxidation ability in the degradation of humic acid than those prepared by ion-exchange method. Although the bulk properties (e.g., light absorbance and crystalline size) are almost the same, it was calculated that the specific surface area of the synthesized Ag_3PO_4 fabricated through precipitation method is nearly 7 times larger than that through the ion-exchange method (8.7 m^2/g and 1.2 m^2/g for precipitation method prepared and ion-exchange method prepared, respectively). In addition, the particle size of the former one is mainly centered on 0.3–0.4 μm, while the latter one is predominantly ranging from 6 to 10 μm. It was reported that the Ag_3PO_4 samples prepared by precipitation method showed 95% DOC removal rate for humic acid degradation after 2 h visible light (λ = 451 nm) irradiation.

3.3. Hydrothermal method

Using hydrothermal method to prepare Ag_3PO_4 photocatalyst is also a noteworthy approach. Hydrothermal method is utilizing the chemical reaction between the reagents at a particular temperature and pressure [82–84]. Owing to the specific condition of this method, it could

Table 1
The synthesized parameters of Ag_3PO_4 with different preparation methods.

Method	Morphology	Synthesis procedure	Experimental conditions	Photocatalytic activity	Ref.
Ion-exchange method	1D hollow porous microrod	Under vigorous magnetic stirring, 0.01 M Na_2WO_4 aqueous solution was added into 0.05 g $AgNO_3$ aqueous solution, then 0.05 M Na_2HPO_4 aqueous solution was added drop by drop into the above solution.	0.2 g photocatalysts were added into 100 mL 8 mg/L Rh B and MO solution, respectively. Light source: 300 W Xe arc lamp.	Rh B was completely degrade within 60 s; MO was completely degrade in 60 s.	[74]
	porous nanotube	40 mL 0.05 M $NaHCO_3$ was added slowly into 1 mmol $AgNO_3$ and 2.0 g PVP mixture solution, and stirring for 1 h at room temperature. Then, collected the precipitates and transferred into 30 mL distilled water. Added 20 mL 0.03 mmol Na_2HPO_4 solution drop by drop (5 s/d) into the above solution under vigorous stirring for 3 h, collect the precipitates and dried at 60°C.	30 mg photocatalysts were added into 50 mL Rh B (10 mg/L) and phenol (20 mg/L) solution, respectively.	Rh B was completely degrade in 8 min; 87% phenol was degrade in 80 min.	[80]
Precipitation method	particle	Under magnetic stirring at room temperature, an appropriate amount of $Ca_{10}(PO_4)_6(OH)_2$ were added into $AgNO_3$ solution (the Ag/P atomic ratio was 3.0).	0.02 g photocatalysts were added into 10 mg/L HA solution. Light source: 300 W Xe lamp	95% DOC was removed after 2 h.	[57]
	cubic enclosed completely by six perfect {1 0 0} facets	0.1 M ammonia aqueous solution was added drop by drop into 0.2 g $AgNO_3$ aqueous solution to form a transparent solution, then added 0.15 M Na_2HPO_4 aqueous solution into the above solution.	0.2 g photocatalysts were added into 100 mL 8 mg/L MB solution. Light source: 300 W Xe lamp.	MB was completely degrade in 3 min.	[78]
	rhombic dodecahedral	0.15 M Na_2HPO_4 aqueous solution was added drop by drop into 0.2 g CH_3COOAg aqueous solution.	0.2 g photocatalysts were added into MO and Rh B solution, respectively. Light source: 300 W Xe arc lamp.	MO was completely degrade in 4 min; Rh B was completely degrade within 4 min.	[79]
Hydrothermal method	tetrapod	2.5 mmol $AgNO_3$ were added in 3 mmol 85% H_3PO_4 aqueous solution, then added 37.5 mmol urea into the above solution. Transferred the resulting precursors into a Teflon-lined stainless steel autoclave and maintained at 80 °C for 24 h.	0.1 g photocatalysts were added into 100 mL 8 mg/L Rh B solution. Light source: 300 W Xe arc lamp.	98% Rh B was degrade after 18 min.	[75]
	irregularly spherical	0.25 M Na_3PO_4 solution was added into 0.75 M $AgNO_3$ solution with vigorous stirring for 10 min, and adjust the pH value by 1 M H_3PO_4 and 1 M NaOH solution. Transferred the above solution into Teflon-lined stainless steel autoclave and maintained at certain temperature for certain time. Variate: temperature (100 °C, 150 °C, 200 °C, 250 °C), pH (3, 5, 7, 9), feedstock concentration (0.75 M, 0.375 M, 0.075 M, 0.00375 M for $AgNO_3$), and reaction time (2 h, 6 h, 12 h, 24 h).	0.15 g photocatalysts were added into 180 mL 0.02 M $AgNO_3$ solution, and purged with helium gas to eliminate air before light irradiation. Kept the temperature of the system around 30 °C by thermostatic circulating water. Light source: 300 W Xe arc lamp.	The initial rate of O_2 evolution determined to be 1156 $\mu molg^{-1}h^{-1}$ and apparent quantum yield at 420 nm amounted to 3.69%.	[81]
Colloidal method	colloidal	0.02 M $AgNO_3$ were added into 0.02 M Na_2HPO_4 aqueous solution, then collect the catalyst and dried at 70 °C for 12 h.	0.125 g photocatalysts were added into 125 mL EY (0.042 mM) and MB (0.05 mM) solution, respectively. Light source: 500 W halogen linear lamp.	EY was completely degrade after 10 min; 90% MB was degrade after 15 min.	[76]
Heteroepitaxial growth	concave trisoctahedral	Ammonia solution was added into 0.2 g $AgNO_3$ aqueous solution, then, the Au@Ag nanorods with high aspect ratio and 0.15 M Na_2HPO_4 aqueous solution was added in order.	0.2 g photocatalysts were added in 100 mL 8 mg/L Rh B solution. Light source: 300 W Xe arc lamp.	Rh B was completely degrade within 3 min.	[77]

Note: Rh B (rhodamine B); MO (methyl orange); PVP (poly vinyl pyrrolidone); HA (humic acid); dissolved organic carbon (DOC); EY (Eosin Y); MB (methylene blue).

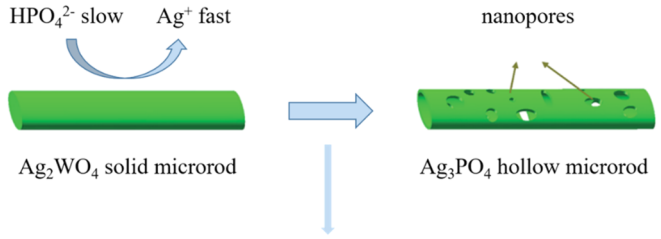

$$3Ag_2WO_4 + 2HPO_4^{2-} = 2Ag_3PO_4 + H_2WO_4 + WO_4^{2-}$$

Fig. 3. Schematic illustration of the ion exchange method: the transfer of Ag_2WO_4 solid microrod to Ag_3PO_4 porous hollow microrod (adapted from Ref. [74]).

replace solid-phase reaction, which is difficult to occur. By controlling the basic synthesis parameter such as hydrothermal temperature and intensity of pressure, Ag_3PO_4 products with few defects, good direction, regular morphology, and high purity could be obtained [75,81,85,86]. The products have superior crystalline and the size is easy to control. Meanwhile, this method is beneficial to the generation of intermediate and special valence state compounds, and could equably realize the doping process, because the atmosphere of surrounding under hydrothermal condition is liable to control. Wang et al. [75] first used this method with the assistance of urea to prepare a highly uniformed Ag_3PO_4 with tetrapod morphology at 2012. Production of tetrapod Ag_3PO_4 undergoes three steps. (i) precipitation process: the addition of urea could neutralize the phosphoric acid to form $H_2PO_4^-$ to react with Ag^+ produce $A_{g3}PO_4$ microrod; (ii) the dissolution process: with the reaction time increase, microrod Ag_3PO_4 would dissolve by the ammonia released from urea hydrolysis; (iii) recrystallization process; through the reaction between dissolved $Ag(NH_3)_2^+$ and PO_4^{3-}, the tetrapod Ag_3PO_4 was shaped up. The uniform tetrapod Ag_3PO_4 possess four cylindrical microrods arms grow along the [110] direction with an average diameter of 5 μm and a length of 15–30 μm, and its specific surface areas is 38.0 m^2/g. The degradation rate of Rh B by as-obtained Ag_3PO_4 particles was more than 2 times higher than the Ag_3PO_4 samples prepared by ion-exchange method. Reaction conditions have been of great influence on the morphology and facets of as-prepared samples. For instance, Cui et al. [87] have discussed the effect of temperature in hydrothermal synthesis procedure of Ag_3PO_4. The authors found out that with the temperature increased from 20 °C to 120 °C, the intensity of (1 1 0) peaks becomes sharper and stronger, which means an increased ratio of exposed {1 1 0} facets. Generally, more exposed {1 1 0} facets means higher photocatalytic activity of Ag_3PO_4, which is conducive to the photocatalytic performance.

3.4. Other methods

Apart from the three methods discussed above, there are still several approaches to prepare the Ag_3PO_4 photocatalyst. For example, Khan et al. [76] synthesized highly active Ag_3PO_4 by the colloidal method. According to their reports, the prepared sample was uniformly spherical-like, and homogeneously in distribution compared to the samples fabricated by precipitation method. The colloidal method created a less concentrated surrounding compared to the precipitation method. In the colloidal method, the reaction limited aggregation played a dominant role, and the cluster-cluster repulsion phenomenon could be conquered by thermal activation process. In precipitation method process (concentrated environment), however, diffusion-limited aggregation results within a short time and the clusters are easier to get close. Samples prepared by colloidal method show 2.6 times higher photocatalytic capacity than that prepared by precipitation method under the same conditions. Surface of photocatalysts is the place where photocatalytic reaction occurred. The more reactive surface, the higher the surface energy. Hence, the facet of Ag_3PO_4 should also be taken into consideration in the synthesis procedure. Jiao et al. [77] firstly fabricated a concave trisoctahedral Ag_3PO_4 microcrystals surrounded by {2 2 1} and {3 3 2} facets through heteroepitaxial growth method. Compared with low-index facets, high-index facets usually equipped with extraordinary density of atomic steps, ledges, kinks, dangling bonds, and higher chemical reaction activities [88]. The samples prepared by this method could thoroughly remove Rh B within 3 min, which is extremely higher than N-doped TiO_2. However, stability of Ag_3PO_4 with high-index facets remains is a problem, which needs further research to remove this roadblock.

3.5. Facet control

There are generally three low-index facets of Ag_3PO_4 (i.e., {1 0 0}, {1 1 0}, and {1 1 1}), which show comparable photocatalytic performance but exhibit better stability compared to high-index facets. The main difference between these three low-index facets of Ag_3PO_4 is the surface states such as the concentration of Ag^+ cations, the concentration of oxygen vacancies, and the concentration of dangling phosphorus-oxygen bonds. For {1 0 0} facets, the proportion of P atoms and Ag^+ cations is 1:2, without any O^{2-} anions in the planes. The enriched Ag^+ cations could be converted to Ag by the photoexcited electrons, which could enhance the separation of photogenerated carries, thereby improving their photocatalytic performance [78]. Additionally, the {1 0 0} facets of Ag_3PO_4 possess a metal-like electronic property, which might be conducive to the promoted harvesting efficiency of photons. Compare to {1 0 0} facets, regular rhombic dodecahedral shaped {1 1 0} facets Ag_3PO_4 had more oxygen vacancies created, more active sites generated, and larger adsorption amounts on these sites on the surface [79]. Wang et al. [75] found that the Ag atoms on the {1 1 0} planes contained threefold-coordinated with one dangling bond and two-coordinated with two dangling bonds, whilst in the {1 0 0} planes, all the Ag atoms were coordinative saturated, which explained the reason for {1 1 0} facets exhibiting the higher reactivity than the {1 0 0} facets. As for tetrahedron Ag_3PO_4 with {1 1 1} facets, the planes consisted of over-abundance of dangling phosphorus-oxygen bonds, which could act as oxidation sites for a better reactivity. Besides, the hole mass along [111] is smaller than other directions in Ag_3PO_4 crystals [89]. That would improve the hole mobility of the tetrahedrons samples, and enhance the separation efficiency, thus improving the photocatalytic activity. It is generally recognized that Ag_3PO_4 exposed with one more of these three facets have great photocatalytic activity, and tetrahedral Ag_3PO_4 with exposed {1 1 1} facets are more photocatalytically active than rhombic dodecahedrals with {1 1 0} facets and cubes with {1 0 0} facets. However. Hsieh et al. [90] demonstrate that there might be controversies about this recognition. The authors tested the photodecomposition capability of MO solution of Ag_3PO_4 with different morphology (cubes, rhombic dodecahedra and tetrahedrons). Interestingly, the results show that the Ag_3PO_4 cubes show the best photodecomposition capability of MO, Ag_3PO_4 rhombic dodecahedra shows a little over half of that, and Ag_3PO_4 tetrahedrons are completely inactive after 90 min of reaction. The authors conclude that this is because {1 1 1} surface have the highest barrier for electron transport to the surface (the most steep upward band bending among these three facets), hence there may no photogenerated electrons and holes arrived in the {1 1 1} faces of Ag_3PO_4 to participate in the photocatalysis. On the contrary, {1 0 0} facet have the least degree of upward band bending, which indicate its have the best electron transmission capacity among these three facets, and the upward bending degree of {1 1 0} facet is between {1 1 1} and {1 0 0} facet, signify less efficiency of photogenerated electron transfer than that of {1 0 0} facet. In addition, Kim et al. [91] exhibit that tetrahedron Ag_3PO_4 have the fastest oxidation capability of amplex red compare to Ag_3PO_4 with mixed facet and cube. The authors state that this is owing to the {1 0 0} facets have coordinatively saturated Ag atoms, whereas the Ag atoms on {1 1 1}

facets are located at three-coordinated sites with one dangling bond. Once the $[Ag_2 = O — Ag]_{surface}$ combined with h^+, the (1 1 1) surface would be less stable than that of (1 0 0) surface, leading to higher recombination rate of photoexcited electrons and holes. To date, there was no consistent recognition of which the crystal structure of Ag_3PO_4 is better for the photocatalytic degradation of pollutants or water splitting, which need researchers put more strength in this aspect in the future study.

4. Summary

The synthesis method plays a significant role in determining the morphology of photocatalysts and its photocatalytic performance. The growth procedure of Ag_3PO_4 was largely rest with the Ag^+ source in ion-exchange method, while in precipitation method was dependent on the PO_4^{3-} source. Thus, the selection of raw material in these methods needs to be carefully considered. As for hydrothermal method, the temperature and time are the key factors that affect the products. It is well known that hydrothermal method could generate materials with high crystallinity, few defects, and regulated morphology [84]. However, the particle size of as-obtained samples was larger than that of prepared at room temperature, the surface area could greatly decrease at hydrothermal temperature, and the yield of this method is quite low. Besides, the operation sequence of this method is more complicated than that of other two methods. In this section, we only briefly introduced some specific features of these methods. In the synthesis process, other influential factors such as the additives and pH should be also taken into consideration. For instance, Sulaeman et al. [92] proved that the content of ethanol as the solvent could influence the Ag/P atomic ratio of Ag_3PO_4, thus influence the formation of Ag vacancies on the surface of Ag_3PO_4. Hsieh et al. [90] confirmed that the formation of $[Ag(NH_3)_2]^+$ complex has great influence for the morphology control of precipitation method. The molar ratio of NH_4NO_3/NaOH/$AgNO_3$/K_2HPO_4 was controlled at 2:1.8:1:2 in a sequence adding order to synthesis Ag_3PO_4 cubes. By adjusting the molar ratio of NH_4NO_4 and $AgNO_3$, the authors successfully fabricate Ag_3PO_4 particles with different morphology (e.g., rhombic dodecahedra, {1 0 0}-truncated rhombic dodecahedra, tetrahedra, and tetrapods). Forming $[Ag(NH_3)_2]^+$ complexes before adding phosphate could strikingly reduce the driving force toward Ag_3PO_4 production, thus efficiently controlled the shape of products. Besides, different morphology of Ag_3PO_4 also was a significant parameter for the photocatalytic activity needs to carefully considered. The porous and hollow structure is conducive to the enhancement of light harvesting, the photogenerated electron-hole separation efficiency, and immersing of reactants to the photocatalysts. In the design stage, researchers should carefully take all these influence parameters into consideration, choose a specific method for a specific purpose. In addition, researchers also should make unremitting efforts to develop simple and green synthesis methods for the full-scale fabrication of Ag_3PO_4 photocatalyst with high photocatalytic performance in the future.

5. What hinder the practical application of Ag_3PO_4?

Ag_3PO_4 is an excellent photocatalyst because it can be excited by visible light and possess strong photooxidation capability. However, to date, application of Ag_3PO_4 in treating organic pollutants in real-world scenarios has not yet been achieved. Thus, one might want to know what hinders the practical application of Ag_3PO_4. There are indeed several barriers that need to be removed. One big challenge is the severe self-photocorrosion, which strongly limits its cyclic utilization. The photocorrosion phenomenon gives rise to a series of severe issues. Firstly, in large-scale applications, consumption of bare Ag_3PO_4 photocatalyst is high because silver is a noble metal. Price of TiO_2 (CODE # 51026962. Sinopharm Chemical Reagent Co., Ltd.) is almost ¥3.75 per gram. However, the price of $AgNO_3$ (CODE # 81012360. Sinopharm Chemical Reagent Co., Ltd.) is approximately ¥10.24 per gram, which means that the price of Ag_3PO_4 is ¥30.72 per gram at least (without considering the cost of PO_4^{3-} source and other additives), which is 8 times more expensive than TiO_2 (CODE # 51026962. Sinopharm Chemical Reagent Co., Ltd.). That makes using bare Ag_3PO_4 as photocatalyst for water purification impracticable. Secondly, Ag_3PO_4 is slightly soluble in water ($Ksp = 1.6 * 10^{-16}$), and dissolved in nitric acid or ammonia solution, thus its reclamation in real-world situation is difficult. Lastly, the photogenerated electrons under light irradiation could be absorbed by the Ag^+ released from Ag_3PO_4, and consequently reduced to metallic silver, which would deposit on the surface of Ag_3PO_4 ($4Ag_3PO_4 + 6H_2O + 12h^+ + 12e^- \rightarrow 12Ag + 4H_3PO_4 + 3O_2$). This is owing to the position of conduction band of Ag_3PO_4 is +0.45 V, which is much more positive than the potential of H_2O/H_2 and more negative than that of Ag/Ag^+, thus the photoinduced electrons would be adopted by Ag^+ released from the lattice of Ag_3PO_4 instead of H_2O if there were no scavengers exist. As a result, the structure of Ag_3PO_4 could be destroyed, and thus the photocatalytic activity would decrease after several photocatalysis reactions, which greatly hindered its practical application. According to the high-resolution Ag 3d XPS spectra of pure Ag_3PO_4 after one run of degradation of Rh B (Fig. 4), Chang et al. [66] calculated that more than 27% of metallic Ag would be formed on the surface of Ag_3PO_4. Teng et al. [65] reported that Rh B was completely degraded by Ag_3PO_4 within 4 min under Xe lamp irradiation. After three cyclic experiments, however, only 34% of Rh B was degraded under the same situation.

6. How to remove these barriers?

6.1. Surface modification

6.1.1. Plasmonic effect

Metal deposition is a commonly used method for the enhancement of photocatalytic performance. There are mainly two mechanisms for the metal/semiconductor composites, namely, Schottky junction and plasmonic effect. Generally, Schottky junction was formed when there is a direct contact between the metal and semiconductor, while the plasmonic effect could influence the charge transfer of semiconductor even there was an insulating interlayer in the middle of metal and semiconductor. While the metal and the semiconductor have matched work functions and were stuck together intimately, a metal-semiconductor Schottky junction was formed, which can facilitate the separation of electron-hole pairs for charge transfer between these components [93,94]. However, improved separation efficiency was cost of the redox ability of carriers. Owing to the difference of Fermi levels of

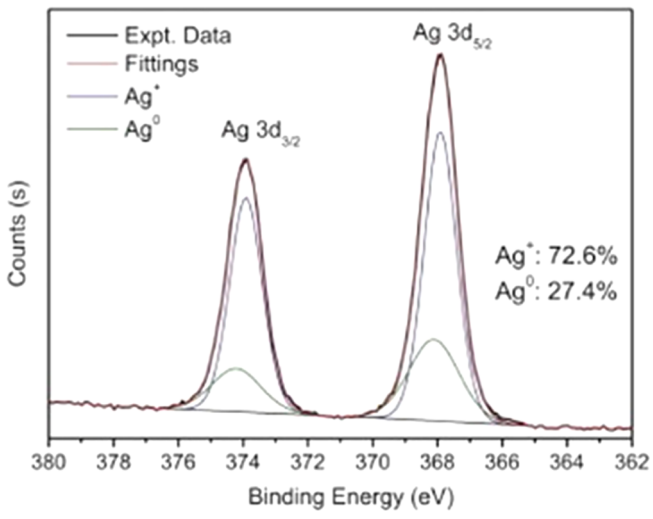

Fig. 4. The high-resolution Ag 3d XPS spectra of pure Ag_3PO_4 after one run of degradation of Rh B (cited from Ref. [66]).

metal and the conduction band of n-type semiconductor or valence band of p-type semiconductor, the energy of carriers was inevitably lost during the transfer process from semiconductor to metal [95]. Normally, the plasmonic metals were defined as Au, Ag and Cu, and the others were generally considered as non-plasmonic metals in the photocatalytic research field [95]. The localized surface plasmon resonance (LSPR) effects could result in collective oscillation of the free electrons, which can induce strong absorption of the electromagnetic energy, hence enhancing the absorption and photocatalytic performances of the semiconductor [96]. For metal/Ag_3PO_4 composites, generally, the electrons would flow into metal from Ag_3PO_4 crystal until it came to the equilibrium of the two systems and formed a new Fermi level as long as the heterostructures were formed. Meanwhile, bands of Ag_3PO_4 bend upward to the surface and an internal electric field directed from Ag_3PO_4 to metal were established. The electrons would accumulate on the metal instead of the surface of Ag_3PO_4, thereby mitigating its photocorrosion. These electrons could merge with the trapped surface oxygen molecules to generate $O_2^{\cdot -}$ reactive species for photooxidation reaction. Moreover, insoluble metal deposited on Ag_3PO_4 could guard the Ag_3PO_4 from dissolution in aqueous solution.

Ag nanoparticles could be generated in both production and photocatalysis processes. In Ag/Ag_3PO_4 composites system, the photogenerated electrons would be transferred to Ag, and the holes remain on the Ag_3PO_4 lattice surface during the irradiation, owing to the existence of PO_4^{3-} ions, thereby boosting the separation efficiency of photoexcited electron/hole pairs and achieving high stability [97]. The main function of Ag in this system is to accelerate the transfer of photoexcited electrons from Ag_3PO_4 conduction band to the Ag nanoparticles and forming O_2^- or $^{\cdot}O_2^-$ reactive species by trapping O_2 and H_2O for degradation of organic contaminants [98]. Ag/Ag_3PO_4 showed a more efficient and stable photocatalytic performance compared to pure Ag_3PO_4 even after five cycles [99]. The XRD patterns of Ag/Ag_3PO_4 after cycling photodegradation experiments (Fig. 5) showed that the change of the phase structure was inappreciable (the content of Ag nanoparticles were 5.73% and 5.84% before and after cycling experiments), and no more Ag nanoparticles were generated. The reduction ability of Ag_3PO_4 could also be promoted by Ag deposition. Patil et al. [100] reported that Ag/Ag_3PO_4 glass nanocomposites could be used for H_2 production from H_2S, with maximum H_2 output being 3920.4 $\mu mol \cdot h^{-1} \cdot g^{-1}$. The overvoltage of hydrogen of Ag metal is −0.22 V vs. NHE, which is more negative compared to pristine Ag_3PO_4 (+0.285 V vs. NHE), which makes the H_2 yield over Ag seems profitable and reasonable. However, in such a composite system, the stability issue was still not fully solved, because some photogenerated electrons inevitably stayed in the conduction band of Ag_3PO_4, which could reduce Ag^+ of Ag_3PO_4 to form metallic Ag.

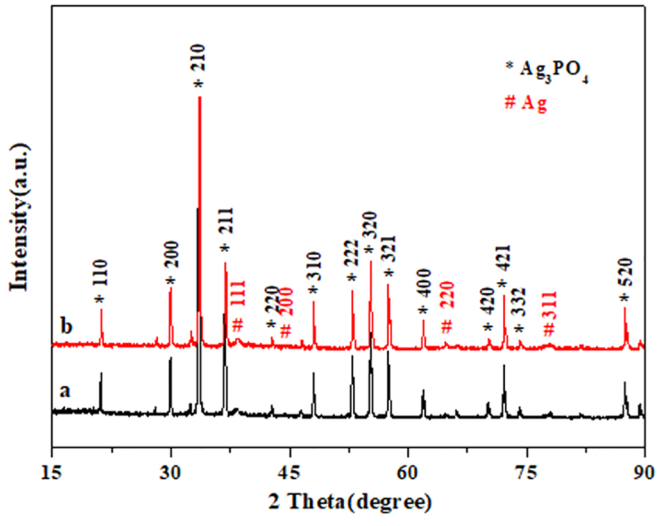

Fig. 5. XRD patterns of (a) Ag/Ag_3PO_4 composite, (b) Ag/Ag_3PO_4 after the 5th cycling photodegradation of Rh B (cited from Ref. [99]).

Apart from Ag, the deposition of other noble metals on Ag_3PO_4 has also been studied by researchers [101–103]. Similar to Ag/Ag_3PO_4, the photoinduced electrons could be accumulated in noble metal through the established electric field between Ag_3PO_4 and noble metal, inhibition of the recombination of photogenerated carriers. The photocatalytic activity of the M/Ag_3PO_4 (M = Pt, Pd, Au) is followed by the order: Pt/Ag_3PO_4 > Pd/Ag_3PO_4 > Au/Ag_3PO_4, which is owing to their different work functions [101]. The larger difference between noble metal and Ag_3PO_4, the faster transformation of electrons from Ag_3PO_4 to noble metal. For Au/Ag_3PO_4, the introduce of Au particles could not only facilitate the electron transfer from Ag_3PO_4 to Au (owing to the higher electrical conductivity) and acting as electron reservoirs to separate the photoexcited charge carriers, but also could extend the light absorption range up to 800 nm. Liu et al. [103] demonstrated that Au nanorod coupled Ag_3PO_4 could completely decompose Rh B dye after 50 min under solar light irradiation, while 78% for the pure Ag_3PO_4 under the same condition. In this composite, the electrons in the 6sp band of Au could transfer to a higher-energy state owing to the surface plasmon resonance (SPR) effect, and react with O_2 to generate $^{\cdot}O_2^-$ radical. Besides, photoexcited electrons in the conduction band of Ag_3PO_4 could transfer into the Au nanorod, consumed by the vacancies of the Au nanorod, thus facilitate the space separation of the photoexcited electrons and holes. Rh B could be efficiently decomposed by the generated $^{\cdot}O_2^-$ and h^+ radicals. In addition, under a 300 W Xe lamp with a cutoff light filter of 645 nm, the as-prepared Au/Ag_3PO_4 samples still show efficient degradation rate of Rh B, which further verified the light absorption range is amplified to 800 nm.

6.1.2. Constructing multiple semiconductor composites heterojunction

Coupling semiconductor with other is a valid way for the enhancement of photocatalytic performance. The hybrid photocatalysts may have complementary features and have optimal performances than single component. The separation and transportation of photogenerated charges could be improved, and semiconductors with larger band gaps could be sensitized through introducing semiconductors with smaller band gaps. Moreover, the stability of semiconductors could be increased by coupling with some semiconductors with superb electrochemical/photochemical stability. During the past decades, numerous studies of semiconductor coupled with Ag_3PO_4 were reported, showing improved separation efficiency of photoinduced charge carriers, strengthened photostability of Ag_3PO_4, enhanced photoreduction ability, and simultaneously increased photocatalytic performance. We simplified present the two types of connection mechanism between semiconductors and Ag_3PO_4 (type II and Z-scheme-like), carbon materials or polymers coupled Ag_3PO_4, and some novel ternary or multicomponent Ag_3PO_4 hybrid composites in this section.

There are generally three types heterostructure based on the bandgaps and electronic affinity of semiconductors, namely, type I (straddling), type II (staggered), and type III (broken) (Fig. 6). The former two types are more commonly used in practical heterostructure devices. For type I, photocatalyst I (PC I) has narrower band gap compare to photocatalyst II (PC II), and both the location of conduction band and valence band of PC I was within PC II (Fig. 6A). This type of heterostructures is conducive to the accumulation of electrons and holes in PC I, and were mostly utilized in optical devices such as light emitting diodes and lasers [104,105]. As for Type II heterojunction, photogenerated electrons in the conduction band of PC I could transfer to the conduction band of PC II, accompanied by the transformation of the photogenerated holes from the valence band of PC II to the valence band of PC I (Fig. 6B). Similar to the Schottky junction of metal/semiconductor composites, in the interface of two semiconductors, a built-in field would be generated, which is conducive to the separation of photoexcited electron-hole pairs in this region, leading to the

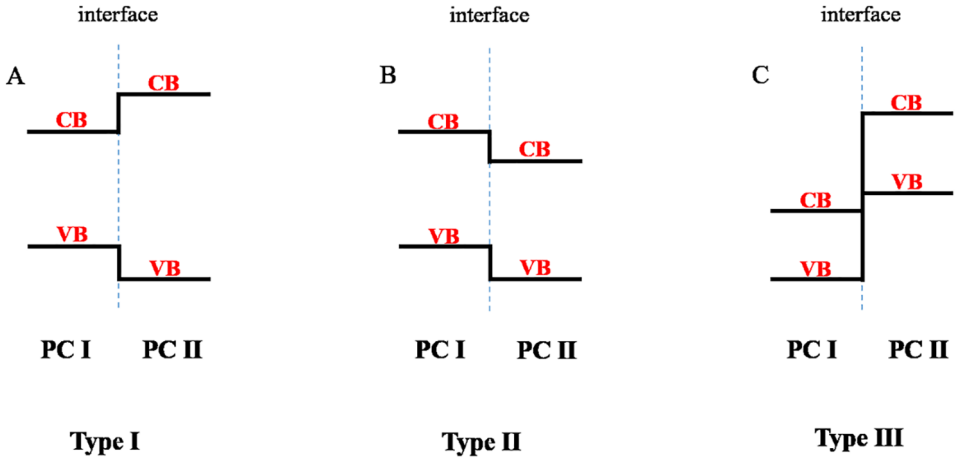

Fig. 6. (A) Type I (straddling), (B) type II (staggered), and (C) type III (broken) heterostructure.

enhancement of photocatalytic performance. The elevated photocatalytic capability could also be attributed to the augmented surface area and enhanced absorption of reactants. Charge transfer directions were depending on the position of the conduction band and valence band of the two semiconductors. In this heterojunction system, we preferred that Ag_3PO_4 to act as PC II to transfer the photoinduced electrons to other semiconductor, which may show a better inhibition capability for the photocorrosion than the type II heterojunction where Ag_3PO_4 act as the PC I. It should be noted that metallic Ag could be still generated in the photocatalysis process, reducing the cyclic utilization capability of Ag_3PO_4. Yao et al. [106] reported that the type II heterojunction Ag_3PO_4/TiO_2 composites showed 90% degradation rate of the methylene blue (MB) after 6 min under irradiation, which was higher than that of Ag_3PO_4 samples. This composite system reduced the loading of metallic Ag from 77 wt% to 47 wt%, which could be regarded as significant progress for reducing photocorrosion phenomenon.

Although the recombination of photoinduced electron-hole pairs is restrained by the type II heterojunctions, the redox ability of the charges in this system is weakened. The Z-scheme-like photocatalytic system may be an ideal candidate to solve this problem [107]. Similar to type II heterojunction photocatalytic systems, the separation of photoexcited electron/hole pairs could be also enhanced in the Z-scheme-like photocatalytic system. Photogenerated electrons in the conduction band of PC I could encounter with the photogenerated holes in the valence band of PC II through either a conductor or a direct contact (Fig. 7 A and B). The photoinduced electrons still remain in the more negative conduction band of PC II for photoreduction process, while the photoexcited holes remain in the more positive valence band of PC I for photooxidation reaction. The driving force energy needed for this system is reduced which could make the hybrid photocatalyst utilize visible-light more efficiently.

Transition metal sulfides (e.g. MoS_2 and WS_2) recently attracted more and more attention from researchers. Considering the band gap energy of transition metal sulfides and Ag_3PO_4, it is reasonable to believe that the composition of these semiconductors could constructing a Z-scheme-like heterojunction, which could effectively restrain the oxidation of transition metal sulfides and the reduction of Ag_3PO_4, hence improve both the photocatalytic activity and stability. The two dimensional graphene-like materials MoS_2 have a suitable band edges ($E_{CB} = -0.12$ V, $E_{VB} = 1.78$ V), which is well matched with Ag_3PO_4 to form Z-scheme-like photocatalytic system [108,109]. Zhu et al. [110] reported that Ag_3PO_4/MoS_2 composite photocatalyst exhibited excellent photocatalytic degradation rate of organic contaminants and ascendant stability according to the recycling experiments. MoS_2 could effectively accept electrons and form strong interaction with Ag_3PO_4. Photogenerated electrons of Ag_3PO_4 could recombine with the photoinduced hole of MoS_2 in Ag particles which were formed by the photocorrosion of Ag_3PO_4. The Ag particles serve as charge recombination center and are favorable to the development of the Z-scheme-like system. The holes remaining in Ag_3PO_4 and electrons in MoS_2 could

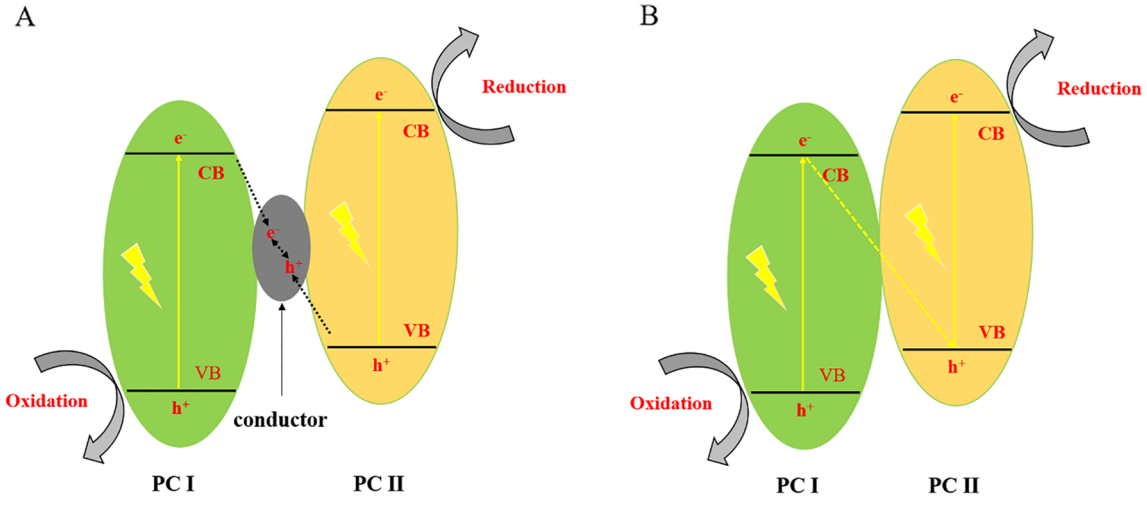

Fig. 7. (A) With conductor and (B) mediator free Z-scheme-like heterostructure.

simultaneously be utilized for the redox reactions. The separation efficiency was improved and the photocatalytic performance was also enhanced.

Metal-free graphitic carbon nitride ($g\text{-}C_3N_4$) is a material with stable, abundant, responsive to visible-light, and exhibits splendid electronic properties. The band gap width of $g\text{-}C_3N_4$ is about 2.7 eV (the conduction band position of $g\text{-}C_3N_4$ is −1.12 V and the valence band position of it is 1.57 V) [18,111–114]. He et al. [115] reported that the Z-scheme-like $Ag_3PO_4/g\text{-}C_3N_4$ composite could transfer CO_2 to fuel. Photoinduced holes in $g\text{-}C_3N_4$ and the photoexcited electrons in Ag_3PO_4 would combine in Ag nanoparticles. The photogenerated electrons in $g\text{-}C_3N_4$ could reduce H^+ or CO_2 while the photogenerated holes in Ag_3PO_4 could be used to oxidize H_2O to O_2 or degrade pollutants. The biggest CO_2 conversion rate of $Ag_3PO_4/g\text{-}C_3N_4$ photocatalyst 57.5 $\mu mol \cdot h^{-1} \cdot g_{cat}^{-1}$, which was almost 6.1 and 10.4 times higher than that of $g\text{-}C_3N_4$ and P25 under the same conditions, respectively.

Besides the two kinds of hybrid mechanisms introduced above, other materials such as carbon materials (e.g., fullerene and graphene) [116,117], polymers [118–121], and metal-organic frameworks [122–124] could be used as the conductor for the improvement of photocatalytic performance. Given credit to the good electron transport of carbon compounds, it may be a kind of the most appropriate material to combine with Ag_3PO_4 [125–127]. In the carbon-based materials, graphydiyne with π-conjugated structure of sp- and sp^2-hybridized carbon atoms have attracted tremendous attention. Its electron and hole mobility is about $2 * 10^5\ cm^2V^{-1}s^{-1}$ [128] and $10^4\ cm^2V^{-1}s^{-1}$ [129] order of magnitude, respectively, and the conductivity of graphdiyne is measured as $2.516 * 10^{-4}$ S/m [130]. The graphydiyne has uniformly distributed pores and a tunable band gap in the range of 0.46–1.22 eV [131]. Guo et al. [132] studied the promoted photocatalytic acitivity of graphydiyne/Ag_3PO_4 pickering emulsion. The abundant butadiyne bonds (−C≡C−C≡C−) makes graphydiyne works as an excellent acceptor (formed a large π-conjugated system) for the photoexctited electrons of Ag_3PO_4, and an appropriate amount of the precursor Ag^+ could be reduced to Ag^0 by the introduction of graphydiyne due to the low work function of it. According to the authors, MB solution could be completely photodegraded within 10 min by this graphydiyne/Ag_3PO_4 emulsion system under visible light irradiation, while only 75% MB were photodegraded by carbon nanotube/Ag_3PO_4 or graphene/Ag_3PO_4 photocatalyst under the same condition.

Coupling Ag_3PO_4 with polymers may be an efficient way to restrain the photocorrosion of Ag_3PO_4, because it could function as a passivation layer to cut down the number of surface recombination sites and prevents the photocorrosion of semiconductor [133]. For instance, Yue et al. [121] synthesized a core-shell structure Ag_3PO_4@benzoxazine soft gel nanocomposite for the improvement of interface properties and stability of Ag_3PO_4. The silver amine complex ion formed through the amino group of benzoxazine and Ag^+ ions on the surface of Ag_3PO_4 could consuming the photogenerated electrons of Ag_3PO_4 with the O_2 molecule absorbed on it surface to produce $^{\cdot}O_2^-$ radicals, thus restrain the photocorrosion of Ag_3PO_4. Besides, the shell of benzoxazine could efficiently inhibit the dissolution of Ag_3PO_4 in aqueous solution, hence promoted the structural stability.

With the development of photocatalysis technology, researchers are no longer satisfied study the binary complex photocatalyst, more and more researchers put their strength on the study of ternary or multi-component hybrid composites. To date, lots of researchers pronounced that using some intermedium such as noble metal [134–139], carbon materials [14,140–142], or polymers [143–145] to accelerate the charge carrier transformation is an efficient way to construct a ternary hybrid composite photocatalyst. For instance, Cai et al. [140] recently synthesized Ag_3PO_4@RGO@La,Cr:$SrTiO_3$ photocatalysts which showed an excellent anti-photocorrosion and photocatalytic performance. The enwrapped RGO is avail for the transfer of charge carriers, and could prolong its lifetime. In addition, it could behavior as sheltering layer to prevent photocorrosion. The as-obtained sample could completely degrade Rh B after 5 min sunlight irradiation, and no loss was detected in the photocatalytic process after 5 cycles. Si et al. [146] reported a Z-scheme-like Ag_3PO_4/graphdiyne/$g\text{-}C_3N_4$ photocatalyst for oxygen evolution. The graphdiyne could boost the oxygen generation by acting as conductive electron mediator bridge as well as to stabilize Ag_3PO_4 as a promising substrate. The O_2 evolution of this composite could reach 753.1 $\mu molg^{-1}h^{-1}$, which is 12.2 times higher than that of pure Ag_3PO_4 photocatalyst.

Shao et al. [143] improved the photocatalytic performance of Ag_3PO_4@benzoxazine by synthesizing Ag_3PO_4 tetrapods with more exposure of {1 1 0} facet and decorated of carbon quantum dots (CQDs) on the surface of Ag_3PO_4. The CQDs could act as an "exciter" by expanding light absorption and strengthening energy conversion via up-conversion photoluminescence effect, thus activate more photogenerated charge carriers from the {1 1 0} facet of Ag_3PO_4 tetrapod. Simultaneously, it could facilitate the electron transfer from the conduction band of Ag_3PO_4 to the conduction band of itself. The silver amine complex formed between Ag_3PO_4 and benzoxazine is beneficial for the free radical chain reaction. This 3D core-shell structure decreased the solubility of Ag_3PO_4. The photocatalytic activity of this composite still remains 95% removal rates of sulfamethoxazole with 10 min even after 9 cycles.

Except the abovementioned ternary Ag_3PO_4 hybrid composites system, other multi-component Ag_3PO_4 hybrid composites were also been studied by researchers. For example, Pan et al. [147] introduced TiO_2 into the laminar $Ag_3PO_4/Ag/MoS_2$ Z-scheme-like heterojunction photocatalyst to prevent the aggregation. Comparing with traditional heterojunctions, the part of $Ag_3PO_4/Ag/MoS_2$ in this composite still forms a Z-scheme-like structure. Additionally, credit to the lamellar structure, the conduction band of MoS_2 may be higher than that of TiO_2, which could lead the photogenerated electrons from MoS_2 transferred into the conduction band of TiO_2, further promote the separation efficiency of photoinduced charge carriers. The photoluminescence of $Ag_3PO_4/Ag/MoS_2/TiO_2$ is obvious weaker than others (Fig. 8), which proved this conjecture. Direct Z-scheme-like photocatalysts for water splitting suffer from charge separation and photocatalytic backward reaction issues [148,149]. Li et al. [150] announced that the synergistic effect of a type II heterostructure could efficiently suppress the backward reaction. The authors deposit Ag_3PO_4 nanoparticles on CeO_2/TiO_2 hierarchical branched nanowires, and speculated that the cascade energy level alignment in CeO_2/TiO_2 hierarchical branched nanowires facilitates the spatial charge separation, thus inhibit the backward reaction, and further improved the photocatalytic activity. Other novel multi-component photocatalytic system such as quasi- type II p-n/n-n dual heterojunction Ag@$Ag_3PO_4/g\text{-}C_3N_4$/NiFe layered double hydroxide (LDH) nanocomposites [151] and dual Z-scheme-like $g\text{-}C_3N_4/Ag_3PO_4/Ag_2MoO_4$ [152] composites were also been investigated by researchers, and their proposed mechanism for charge transfer pathways (including the abovementioned $Ag_3PO_4/Ag/MoS_2/TiO_2$ and $Ag_3PO_4/CeO_2/TiO_2$) were show in Fig. 9.

6.2. Doping

Introducing heteroatoms into the lattice of host material is considered as an excellent way to adjust the photocatalytic performance of semiconductors. Unlike surface modification such as metal deposition, doping is a physical or chemical method, which introduces ions into the internal of host material lattice. It could efficiently modify the surface structure of host material, form some defects (acting as capture centers to inhibit the recombination of photoinduced electron/hole pairs), increase some spectral response, cause significant changes in the band gap (introducing levels), influence the kinetic state of photoinduced charge carriers (causing linear expansion of the transition of charge carriers, and prolong the life time of photoinduced charges), hence is conduced to the improvement of photocatalytic performance [153–156]. However, doping does not always play a positive role in

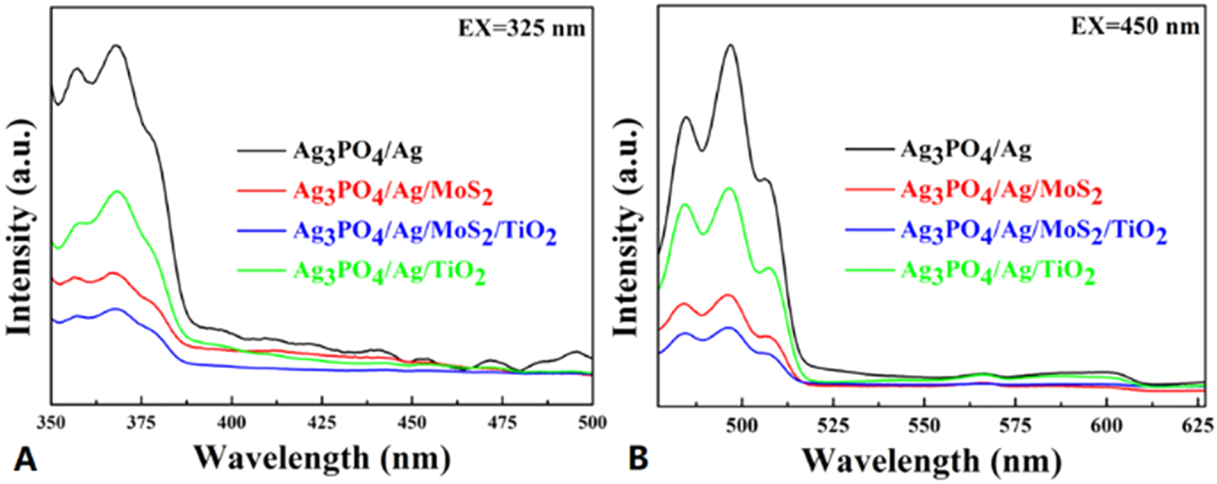

Fig. 8. The photoluminescence of the samples with different excitation wavelength, (A) 325 nm, (B) 450 nm (cited from Ref. [147]).

energy band engineering. Dopants could act as carrier recombination centers when the concentration of dopants exceeds the optimum value, and thus decrease the photocatalytic properties. Doping could also destroy the local symmetry, and the chemical mismatch between the dopant and host may result in the formation of deep defect levels [157]. Therefore, choosing proper dopants for precise engineering the energy band configuration is at a camera position.

Generally, doping could introduce an impurity level or replace some elements in the original crystal. For instance, an impurity energy band would be formed in the doping process of Ni^{2+}-doped Ag_3PO_4 [158]. The additional Ni^{2+} could facilitate the utilization of photons as well as the separation efficiency of photoinduced charge carriers. The

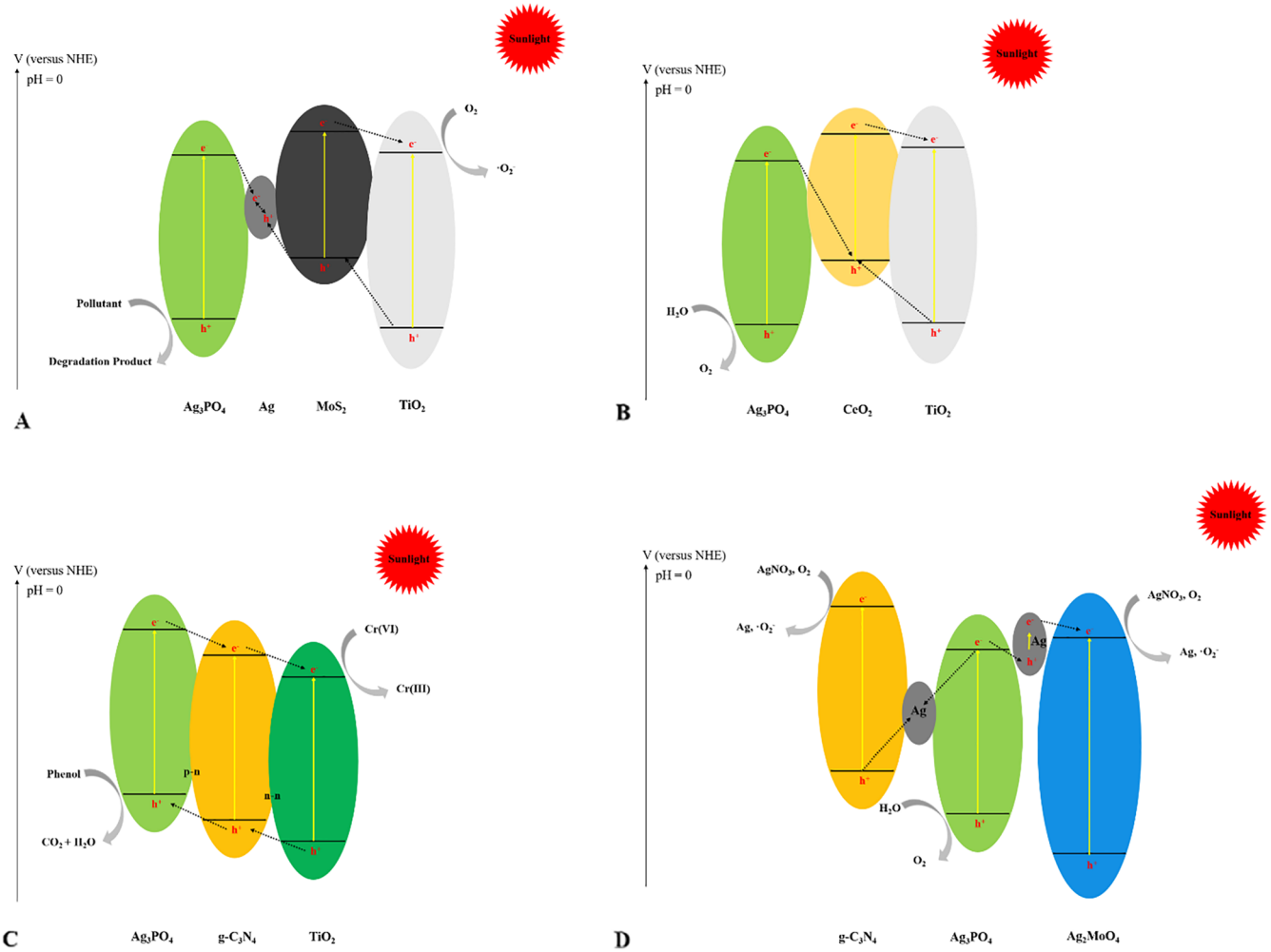

Fig. 9. The proposed mechanism for charge transfer pathways (A) $Ag_3PO_4/Ag/MoS_2/TiO_2$ (adapted from Ref. [147]), (B) $Ag_3PO_4/CeO_2/TiO_2$ (adapted from Ref. [150]), (C) $Ag@Ag_3PO_4/g\text{-}C_3N_4$/NiFe LDH (adapted from Ref. [151]), (D) $g\text{-}C_3N_4/Ag_3PO_4/Ag_2MoO_4$ (adapted from Ref. [152]).

photodegradation rate of methyl orange (MO 40 mg/L) could be reached at 89% by Ni^{2+}-doped Ag_3PO_4 after 4 min under visible light irradiation, whereas 12% of MO (40 mg/L) was only degraded by pure Ag_3PO_4 photocatalyst under the same situation. Five cycling experiments showed that the photodegradation rate of MO (20 mg/L) was still up to 92%. The introduction of copper atoms could substitute silver atoms in the crystalline lattice of Ag_3PO_4, thus create defects that influence the structural ordering, stabilize the cubic structure, and prevent the reduction of Ag^+ by acting as recombination centers to trap photogenerated electrons [159]. Introducing Bi^{3+} ions could replace the P^{5+} ions of Ag_3PO_4 [160]. The valance band level of Ag_3PO_4 could be decreased by bismuth doping, and the band gap energy of Bi^{3+}-Ag_3PO_4 could be reduced to 1.954 eV. Doping Bi^{3+} ions in Ag_3PO_4 suppressed the formation of excess OH defects. High-concentration OH defect is not good for the electronic transitions, and could destroy Ag-O bonds in Ag_3PO_4 to accelerate electronic recombination. Notably, in an aqueous solution, MO molecules carry a negative charge while the Bi^{3+} ions carry a positive charge in doped Ag_3PO_4. Hence, adsorption capability could be accelerated because of the internal attraction between these two groups, which facilitated the photocatalytic reaction. P (V) of Ag_3PO_4 could be substituted by Mo (VI) cations, and new intermediate levels in the forbidden band would be formed after doping procedure of molybdenum [161]. Electronic repulsion capability of Ag_3PO_4 could be improved by Mo doping due to the Mo (VI) cations are more positive than the P (V) cations. Mo doping could break in degeneracy in the Ag 4d orbitals, and Mo 4d orbitals in the conduction band provokes the decrease of the band gap value. Appropriate amount of Mo doping could create an appropriate amount of defects, which could serve as traps to delay the recombination of charge carriers, and forming intermediate states in the forbidden band to lower the E_g. The E_g could be reduced to 2.07 eV for 0.5% Mo doped Ag_3PO_4, and shows two time faster degradation rates than pure Ag_3PO_4 microcrystals toward Rh B solution.

Lanthanides doped semiconductors could form crystalline defects, which could enhance visible wavelengths emission and inhibit the recombination of photogenerated electron-hole pairs [156]. The surface structure of Ag_3PO_4 could be affected by La doping [162]. As the concentration of La dopant increased, more surface defects and pores would be generated. Enhanced photocatalytic capability of La-doped Ag_3PO_4 was aided by the increased porosity, surface defects, and surface area. Other lanthanides like Dy or Er doped Ag_3PO_4 were also be reported [163,164]. Gadolinium cations could replace Ag^+ ions for the Gd-doped Ag_3PO_4 photocatalysts [164]. The M^{3+} (M = Gd, Dy, and Er) ions in this system combined with an electron to form M^{2+}, which would further react with O_2 to increase the formation of $^{\cdot}O_2^-$.

Ba-doped Ag_3PO_4 hollow nanosheets with high photocatalytic activity and photoconversion efficiency were synthesized by Yu et al. [165] via a one-step cation exchange method. This synthesis method was conducive to the dispersion of Ba^{2+} ions. Ba-doped Ag_3PO_4 could completely degrade Rh B solution within 5 min and MO solution in 2.5 min, which was more active than that of cubic or spherical Ag_3PO_4 particles. After five cycling runs, the time for complete degradation was in the range of 5–7 min for Rh B, and 2.5–4 min for MO. Ba doping might greatly increase the amount of oxygen defects, which could inhibit the recombination of the photoinduced charge carriers. An alternative explanation was that doping Ba in the Ag_3PO_4 created a charge imbalance, which caused more OH^- to trap more holes, thereby restraining the recombination of charge pairs and generating more $^{\cdot}OH$.

To date, some cationic metal (e.g. Ni, Bi, Ba, Cu, Mo, La) has been successfully doped into Ag_3PO_4 lattice, and effectively enhanced the photocatalytic performance. However, the metal doping generally introduce localized energy levels in the band gap to modification host material, which may also bring the risk of impairing charge separation and transport by acting as a recombination center. In this regard, one might want to know the anionic nonmetal doping behavior in Ag_3PO_4 since there are plenty of convincible research paper proved the anionic nonmetal doping in TiO_2 and other photocatalytic could obtain a better photocatalytic performance [166–168]. Recently, a fluorine-doped Ag_3PO_4 photocatalyst with boosting activity and stability by a facile in-situ fluorination was reported by Li et al. [169]. Doping F elements with moderate amount have no effect on the basic crystal structure of cubic Ag_3PO_4 and did not introduce impurity phases. Besides, the average crystallite size and crystallinity was improved when the fluoride ions was introduced into Ag_3PO_4, which is benefit for the dissolution and recrystallization processes. Higher crystallinity degree in conducive to the suppressing of bulk charge recombination, and promoting charge separation and transportation. Most of F^- ions would substitute O^{2-} ions in Ag_3PO_4 lattice, and forming a stronger P-F bond compare to the P-O bond. The Fermi level of F-doped Ag_3PO_4 would move toward the conduction band, which is in favor of the charge separation. Small amount of fluorine would adsorbed on the surface of Ag_3PO_4, and absorb more H_2O owing to the fluorine induced $-F\ldots(H-OH)_x$ group involving hydrogen-bonding interactions. F doping would induce more surface defects such as oxygen vacancies, which enhance the capture of surface O_2 as well as the activation of O_2 by photoinduced electrons. In addition, the band gap of F-doped Ag_3PO_4 was raised. Accordingly, the band gap of Ag_3PO_4 and F-doped Ag_3PO_4 is about 2.41 eV and 2.44 eV, respectively. The reduction potential of photogenerated electrons was enhanced and oxidation potential of photogenerated holes was reduced in the F-doped Ag_3PO_4.

Owing to the strong P-O bond, incorporating S into Ag_3PO_4 lattice is difficult, which need much energy input to inset those dopants into PO_4 matrix. Therefore, some researchers proposed using oxoanion groups to modulate semiconductor to get an enhanced photocatalytic activity as an alternative way [170,171]. Cao et al. [172] successfully doped SO_4^{2-} ions into Ag_3PO_4 lattice by a precipitation method. It was feasible to replace PO_4^{3-} by SO_4^{2-} experimentally because the ionic radius of SO_4^{2-} and PO_4^{3-} are similar (0.218 nm of SO_4^{2-} and 0.230 nm for PO_4^{3-}). The S element in SO_4^{2-} had strong electronic interactions with Ag, P and O elements. Give credit to the higher electronegative of S compared to the P atom, the additional SO_4^{2-} would decrease the electron densities around Ag and P elements. Doped SO_4^{2-} created impurity states were mainly distributed in the valence band region, and no impurity state appeared in the forbidden band gap. The Fermi level of SO_4^{2-}-doped Ag_3PO_4 was significantly shifted towards the conduction band. As the concentration of dopant increased, both the VBM and the CBM gradually shifted towards lower energy regions, which were conduced to the enhancement of oxidative capability of photoexcited holes and suppressed the reduction capability of photoexcited electrons. The photodegradation rate of Rh B solution of SO_4^{2-}-doped Ag_3PO_4 was 4.5 times higher compared to Bi^{3+}-doped Ag_3PO_4. Although the photodegradation rate slightly decreased after two cycling runs, the degradation of Rh B solution is still up to 98% after six cyclic runs. Luo et al. [173] proposed a doughnut-like carbonate-doped Ag_3PO_4 with high photocatalytic activity through an ion-exchange method. Similar to the Ba-doped Ag_3PO_4 aforementioned, the authors took advantage of the lower solubility of Ag_3PO_4 ($K_{sp} = 1.4 * 10^{-16}$) compared to Ag_2CO_3 ($K_{sp} = 8.45 * 10^{-12}$) to get a hollow hexagon doughnut-like structure. The CO_3^{2-} doping introduced impurity levels which could narrow the energy gap of Ag_3PO_4 and enhanced its photocatalytic activity. Photoexcited electrons and holes can be efficiently separated and migrated through CO_3^{2-} doped doughnut-like Ag_3PO_4. The photodegradation rate of Rh B solution still maintained 85% of its original activity after five cyclic running.

7. Summary

In this section, we systematically discussed various strategies to enhance photocatalytic performance of Ag_3PO_4, including the deposition of metals, combination with other semiconductors, and doping specific amount of elements into the lattice of Ag_3PO_4. The main purpose of these methods was to boost the separation/transition efficiency

of photoexcited electron-hole pairs, and inhibit its recombination. These methods provide efficient ways to overcome the photo instability and improve the photocatalytic performance of Ag_3PO_4, as well as prevents the dissolution of Ag_3PO_4. Metal/Ag_3PO_4 hybrid photocatalyst provide a solid way to enhance the photostability of Ag_3PO_4. To date, however, most of the researches published only focused on the plasmonic effect of Ag/Ag_3PO_4 composite, other nonplasmonic metals were barely studied. We hope that researchers would put more strength in that aspect, and put forward some other metal/Ag_3PO_4 hybrid photocatalyst with high photostability and photoactivity for practical application. Besides, for the metal/semiconductor system, the particle size, shape, and surrounding environment has a large influence of the plasmonic bands of metal nanoparticles, which also need researchers spend time on the study of the aspect in the future.

Constructing enhanced photocatalytic performance of Ag_3PO_4 based hybrid photocatalyst usually relies on the matched band structures which improve the separation efficiency of photogenerated charge carriers, and the synergistic effects on the aspect of improved visible light absorption and reactants adsorption. Given the high cost of raw material of Ag_3PO_4, decorated small number of Ag_3PO_4 with other inexpensive materials could efficiently cut down the cost, which seems to be a promising way for the industrial application of Ag_3PO_4. However, studies of semiconductor/Ag_3PO_4 were still in its primary stage, only few researchers have put attention on the combination of metal or semiconductor with a specific facet of Ag_3PO_4, as well as the homojunction of Ag_3PO_4. For instance, researchers demonstrated that TiO_2 with well-defined {1 0 1}/{0 0 1} facet junction (p-n junction) of epitaxial interface is conducive to the separation, transfer and surface reaction of charge carriers for more efficient photocatalysis reaction [86]. This also could be an efficient way for the enhancement of photoactivity and stability of Ag_3PO_4. Recently, Xie et al. [174] constructed an Ag_3PO_4 morphological homojunction with enhanced photocatalytic activity. The Ag_3PO_4 homojunction consist of submicron spherical and rhombic dodecahedron particles, introduce an internal field between them, which facilitates the transfer of charge carriers and separation of photoinduced electron-hole pairs. However, the authors were using a simple physical combination process to synthesize the Ag_3PO_4 homojunction, a more sophisticated method and explanation for the homojunction of Ag_3PO_4 should be further studied. In addition, the structures of metal or semiconductor modified Ag_3PO_4 also is a vital parameter for the photocatalytic performance. Numerous structures were proposed to further enhance the photocatalytic activity. For instance, one-dimensional necklace-like Ag nanowires/Ag_3PO_4 cubes were fabricated by Bi et al. [175] in 2012. The authors compared the photocatalytic activity of this composite with core-shell coaxial hetero-nanowires Ag/Ag_3PO_4 and pure Ag_3PO_4 by the degradation of Rh B. The degradation results shows that the necklace-like Ag nanowires/Ag_3PO_4 cubes only need 2 min for the complete degradation of Rh B, while the core-shell coaxial hetero-nanowires Ag/Ag_3PO_4 and pure Ag_3PO_4 need 6 and 8 min, respectively. Improved photocatalytic activity could attribute to the effectively export of enriched electrons on the Ag nanowires and the remained high concentration of holes on Ag_3PO_4 cubes. The position and number of Ag_3PO_4 cubes could be easily controlled in this composite. Novel collective photocatalytic properties could be achieved by the necklace-like structure. Research on novel structure such as isolated structure, multi-segmented heterojunction structure, porous core-shell structure half core-shell stack structure of Ag_3PO_4 should not be ignored in the future studies. In addition, discussion of multiple hybrid composites should also take into consideration. For instance, Zhu et al. [176] successfully synthesized P/Ag/Ag_2O/Ag_3PO_4/TiO_2 composites. The authors declared that the photogenerated electrons of Ag_3PO_4 and Ag_2O in this composite could flow to the Fermi level of Ag, while the photoexcited holes of TiO_2 and Ag_3PO_4 could transfer to the valence band of Ag_2O under sunlight irradiation. In addition, the SPR effect of Ag could lead to generation of energetic electrons, and injected to the TiO_2 to produce superoxide anion radicals and holes for the improved photocatalytic activity of this composite. Thus, the recombination rate of electron-hole pairs was largely decreased, and the photocatalytic activity and stability were largely enhanced.

There is no doubt that doping is an efficient way for the modification of Ag_3PO_4. Doping appropriate amount of dopants into Ag_3PO_4 could efficiently affect the light absorption as well as the charge dynamics. However, there are still some shortcomings in this method. For example, it is hardly to obtain a high doping level owing to the difference of ionic radii of doped and host ions. Dopants could serve as recombination centers, and decrease the redox capability while the use of dopants is introducing electronic states under the CBM or above the VBM. It is worth mentioning that doping method like the aforementioned Ba-doped Ag_3PO_4 and CO_3^{2-}-doped Ag_3PO_4 represents a simple and effective way for the full-scale fabrication of photocatalysts with morphology control and elements doping. In addition, the selectivity of modified Ag_3PO_4 also needs to be taken into consideration. For instance, the CO_3^{2-}-doped Ag_3PO_4 could completely degrade Rh B solution within 8 min and MO within 14 min [173]. This is also important for the practical application of Ag_3PO_4. Moreover, to date, researches about element doped Ag_3PO_4 are really lacking, especially for the nonmetal doped Ag_3PO_4 and co-doping effect, which needs researchers investigated more at this side, and hopefully researchers could summarize general rules for the doping effect of Ag_3PO_4. Furthermore, combined Ag_3PO_4 with other doped materials were abundant studied in the past decade. However, combined doped Ag_3PO_4 with other materials were barely reported, which seems to be a notable aspect for the modification of Ag_3PO_4 photocatalyst.

8. Photoreactors

Another critical issue in the application of photocatalysis is the designing of photoreactors with satisfactory performances at full-scale. Undoubtedly, photocatalysis is a potential pollutant treatment technology. Subramanism et al. [177] calculated that up to 23,000 dollars could be saved by using a submerged membrane photoreactor with flux of 4000 $L/m^2 \cdot h$, and the demand for floor space of submerged membrane photoreactor is much smaller than the traditional aerobic/anaerobic ponding system. Up to now, several kinds of photoreactors have been developed, which all exhibit excellent photocatalysis performance. The first solar photoreactor designed for photocatalytic applications is parabolic trough reactor (PTR, Fig. 10A) which installed in Albuquerque (New Mexico, USA) back in 1989 which could concentrated the sunlight about 50 times on the photoreactor, and was used to treat polluted water containing chlorinated solvents and heavy metals [178,179]. Accordingly, chromium (IV) [180], dichloroacetic acid [181], phenol [182], 4-chlorophenol [183], dichlorophenol [184], pentachlorophenol [185], atrazine [183], and industrial wastewater [186] was successfully degraded by PTR. It favors mass transfer and could avoid possible photocatalyst sedimentation problems. Besides, PTR is a sealing system, and that means no evaporation of volatile compounds. However, there are certain disadvantages about this reactor. First, PTR can only make use of direct solar radiation, suggesting that it is practically useless on cloudy days. Second, the need of tracking system makes it usually expensive to install. Third, optical and quantum efficiency of PTR is low owing to the high recombination rate of electrons and holes. Last, concentrated solar radiation could make the reactor overheating, which can be problems for the efficiently photocatalytic decomposition of pollutants [187–189].

Non-concentrating reactors (NCRs, Fig. 10B) are static system without solar tracking system. The NCRs are able to capture diffuse light, which makes it more efficient compare to PTR. An experiment in Germany shows that for photosensitized cyclization of 1,1-dicarbonitrile under partly sunny or cloudy conditions confirmed this conclusion [190]. The NCRs are simpler systems, which mean that the manufacturing and maintenance cost is lower than that of PTR, makes it effective for small-scale operations [191]. However, the NCRs usually

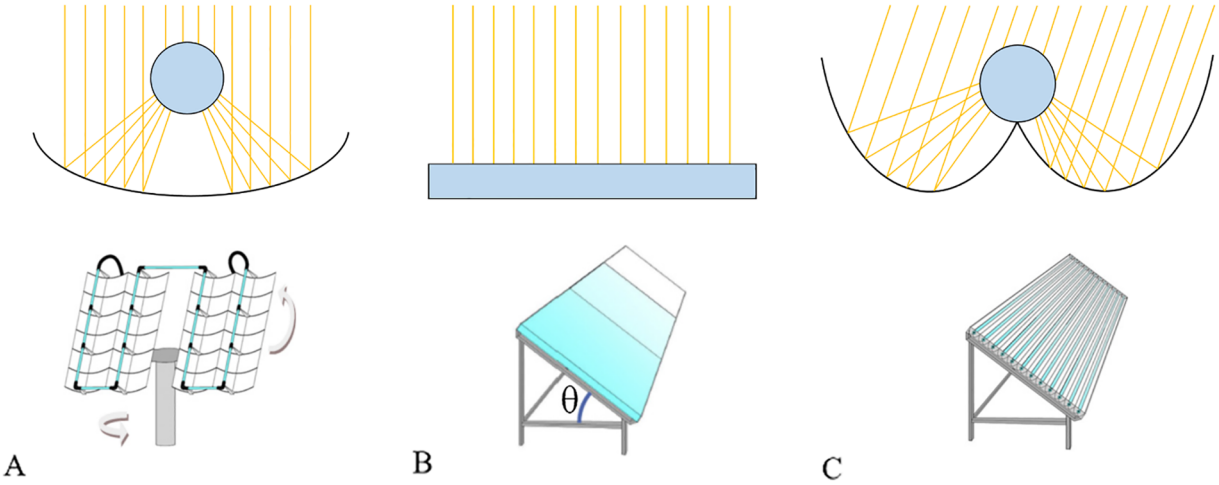

Fig. 10. Schematic drawing of (A) parabolic trough reactor, (B) non-concentrating reactor, and (C) compound parabolic collecting reactor.

work with laminar flow, which could cause mass transfer problems in photocatalysis and oversized floor space. In addition, the NCRs usually are open systems may lead to a highly volatile chemical and water loss by evaporation.

Compound parabolic collecting reactors (CPCRs, Fig. 10C) are stationary reactors with a parabolic reflective surface around a cylindrical reactor tube. It has both advantages of PTR and NCR. CPCR is a low concentrating system without solar tracking system, which significantly decreases the costs and complexity of this system. The reflective surface could reflect indirect light onto the reactor tubes, thus make it capture both direct and diffuse sunlight, as well as makes the reactor volumes smaller. The sanitary landfill leachate [192], olive mill waste [193], urban wastewater [194], toxic compounds such as pathogenic organisms [195], pesticides [196], chlorinated solvents [197], and biorecalcitrant compounds [198,199] could be removed from water by this photoreactor.

Except the abovementioned three photoreactors, several kinds of pilot photoreactors have been developed, which exhibit satisfactory photocatalysis performances at bench-scale. For instance, Abdel-Maksoud et al. [200] designed a tray photoreactor (Fig. 11A) based on using the sand supported TiO_2 as photocatalysts for the degradation of phenol. The reactor is operated in a recirculating batch mode. The liquid could be recirculation pumped into the central vertical feeder which passes through the tray center. The inverted nozzle makes sure a radial flow of water along the tray. The tray side has 20 v-notch weirs which participate in the photocatalytic reaction. By subtly control the recirculation flow rate, formed polluted liquid film over the tray does not hinder the efficient light penetration. After the photocatalytic treatment, the liquid would fall down to the tank bottom ensuring water oxygenation, participate in the loop until it hit the water quality standards. This tray photoreactor is suitable for scale-up and commercialization owing to it modular design, integrated storage, and ease of continuous mode operation. Mosleh et al. [122] successfully applied Ag_3PO_4/AgBr/Ag-HKUST-1-MOF photocatalysts in a continuous flow photocatalytic rotating packed bed (Fig. 11B) for mixture dyes (methylene blue, auramine-O, and erythrosine) photodegradation under blue LED light irradiation. The degradation efficiency of these three dyes is 92.01%, 89.96%, and 89.57%, respectively. The optimum operating parameters are as follows: 75 min of irradiation time, 15 mg/L of each dye, 0.4 g/L of photocatalyst, 100 rpm of rotational speed, 0.3 L/min of solution flow rate and 25 L/min of aeration rate. The composite photocatalyst shows high stability under repeated photocatalytic reaction for 5 times. Besides, this photocatalytic reactor has less physical size and volume than conventional photocatalytic reactor because of the higher interfacial surface created by the device and highly efficient photocatalyst. The packed catalyst saves the cost of the filtration stage and avoids emission of Ag_3PO_4/AgBr/Ag-HKUST-1-MOF photocatalysts.

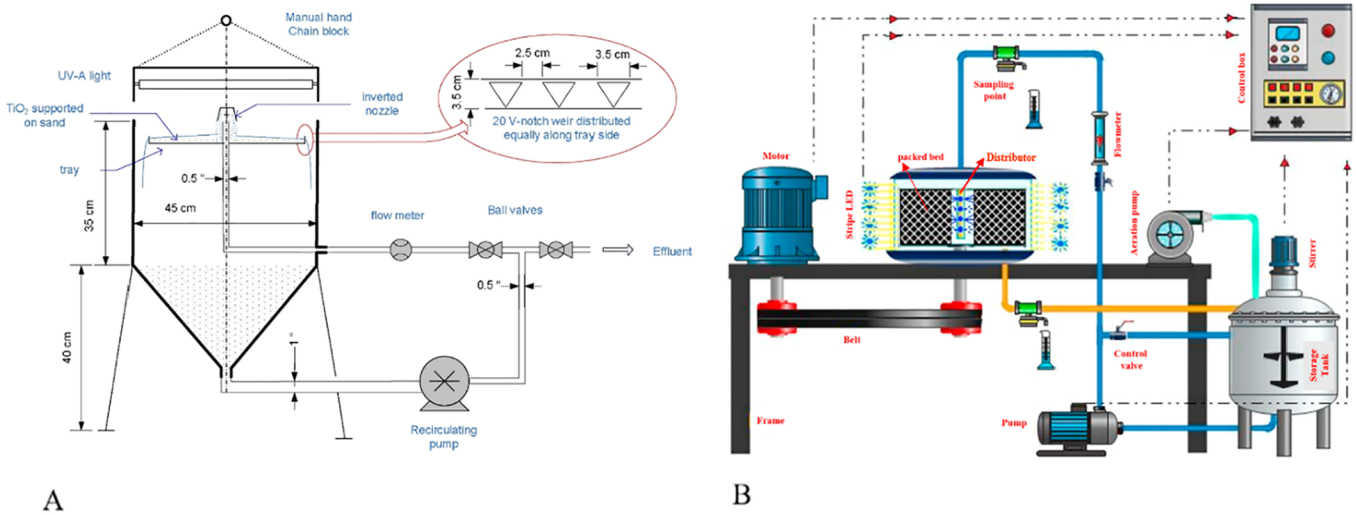

Fig. 11. (A) The tray photoreactor (cited from Ref. [200]) and (B) the rotating packed bed photocatalytic rector (cited from Ref. [122]).

There are mainly two ways to use the photocatalysts in these reactors, i.e., using nanosized powder-like photocatalysts and using immobilized photocatalysts. The nanosized powder-like photocatalysts were often utilized in laboratory experiments, and was generally removed through precipitation or filtration methods. The reactors with dispersed photocatalysts have low pressure drop, large contact surface area for adsorption and reaction, and effective mass transfer of contaminants to nanosized powder-like photocatalysts [201]. However, the stirring of treated water and separation of nanosized powder-like catalysts from it after each run is difficult to be achieved, which greatly hinder its practical application in real-world wastewater situations. Lee et al. [202] successfully separated nanosized powder-like TiO_2 photocatalysts dispersing in water by an optimal coagulant dose, proper flocculation, and sand filtration measurements. However, these methods are complicated, costly, and time consuming. For photocatalysis reaction, small particle sizes generally mean high photocatalytic activities, but smaller photocatalysts suspended in water are not easy to remove and recycle, and may permeate through filtration materials and block filter membranes. Combined Ag_3PO_4 with magnetic materials such as Fe_3O_4 [203,204], $MnFe_2O_4$ [205], and $NiFe_2O_4$ [206] appears to be an efficient way for the recycling of Ag_3PO_4 based composite photocatalysts. The magnetic composite could be totally separated from the solution by an extra magnetic field, which much simplified the recycle process.

For full-scale applications, immobilized photocatalysts seems to be a solution to avoid the recycle problem, but previous publications showed that the photocatalytic performance decreased significantly, as compared to the nanosized powder-like photocatalysts owing to the much smaller contact surface [207,208]. Therefore, it is vital to develop novel immobilized photocatalysts with enough photocatalytic activity for the pollutant treatment. Chen et al. [134] synthesized 3D graphene aerogels/Ag/Ag@Ag_3PO_4 heterostructure photocatalysts for the efficient adsorption-photocatalysis of different dyes in water. Graphene is an ideal supporting material for the construction of Ag_3PO_4 based composite photocatalysts. The macroscopic porous structure of 3D graphene aerogels makes it an easy and convenient recycling support for semiconductor photocatalysts. At the end of a photocatalytic cycle, workers could simply use tweezers to take out the photocatalyst, and could be employed into another phtocatalytic cycle after rinsing. Zhu et al. [176] synthesized a novel P/Ag/Ag_2O/Ag_3PO_4/TiO_2 composite film on the inner-surface of glass tube for circulatory water purification and antibacterial application under solar light irradiation. The degradation rate of Rh B of this composite could reach 99.9% after 60 min, and showed no attenuation of degradation rate even after five recycling runs. Qu et al. [144] fabricated sandwich structural Ag_3PO_4 nanoparticle/polydopamine/Al_2O_3 porous small balls with excellent photocatalytic activity under natural irradiation. The role of polydopamine in this composite is to adhere between Al_2O_3 and Ag_3PO_4, and reduce a small part of Ag_3PO_4 to metallic Ag nanosphere for increased specific surface area and enhanced photocatalytic activity. The porous Al_2O_3 plays the role of the substrate for the Ag_3PO_4/Al_2O_3 heterojunction, and increase the specific surface area of this composite. The authors calculated the natural light intensity in an ordinary sunny day was 220 lx, which is 1/5 than that of 90 mW/cm^2 Xe lamp and 1/9 than that of 180 mW/cm^2 Xe lamp. In the natural irradiation, 5 ppm of MB, Rh B, and orange II could be completely degraded in 40, 60 and 30 min, respectively. Besides, the superhydrophilic surface of this composite provide an excellent antioil property, which greatly reduces secondary pollution, and a small ball structure photocatalyst is much more easy to use and recycle. In addition, membrane is a monolithic material, which is easy to recycle in aqueous solution. The photocatalytic performance of Ag_3PO_4 based composite photocatalyst membranes such as Ag_3PO_4/polyacrylonitrile composite electrospun fiber membranes [119,209,210] and multi-wall carbon nanotubes/Ag_3PO_4/polyacrylonitrile ternary composite fiber membranes [211] were also been studied in detail.

Compare to nanosized powder-like photocatalysts, we believe that immobilized photocatalysts are the main direction of development of photocatalysis due to it recycle capability is much better than the nanosized powder-like photocatalysts. Researchers should put more strength to create immobilized photocatalysts with high photocatalytic performance. Except the innovation of Ag_3PO_4-based photocatalyst, designing suitable photoreactor for the pollutant treatment also is a vital aspect that worthy of attention. Researchers should design photoreactors which suitable for the real-world situation as well as combine the characteristics of photocatalysts for better photocatalytic performance. It is interesting to note that most researchers are focused on the study of the innovation of Ag_3PO_4-based photocatalyst to restrain its photocorrosion, and very few researchers have to keep an eye on the rejuvenation of Ag_3PO_4-based photocatalyst. The photocorrosion phenomenon is inevitable for any of Ag_3PO_4-based photocatalyst participated photocatalytic reaction. Until now, we only know that H_2O_2 could served as the chemical oxidation to reinsert the Ag^0 into the Ag_3PO_4 photocatalyst ($6Ag + 3H_2O_2 + 2H_PO_4^{2-} \rightarrow 2Ag_3PO_4 + 2H_2O + 4OH^-$), and controlled the morphology of the regenerated photocatalyst owing to its pH variation ability which influences nucleation and growth. We hope that researchers could pay great attention to this field, and report novel rejuvenation methods for Ag_3PO_4-based photocatalyst.

For the better photocatalytic performance, combine photocatalysis with other pollutant treatment methods seems to be a valid way. For instance, Almomani et al. [212] proved that combining solar photocatalytic oxidation process with ozonation could significantly enhanced the removal performance of non-biodegradable pharmaceuticals, increased the degree of mineralization, reduce the chemical requirements, and reduced the demand for ozone and energy through the tested performance of a pilot plant for the treatment of wastewater containing emerging contaminates. The photogenerated electrons accumulate on the conduction band of Ag_3PO_4 could react with O_2 and H^+ to form H_2O_2 (0.68 V vs NHE). However, the generated H_2O_2 can hardly be used in the photocatalysis process. Even more, at a low concentration, the H_2O_2 could consuming the photoinduced holes, which has been demonstrated as the main active specials in the pollutant photocatalysis process of Ag_3PO_4. Hence, how to turn the disadvantages into advantages of Ag_3PO_4 is a big challenge for researchers. Huang et al. [206] fabricated a Z-scheme-like Ag_3PO_4@$NiFe_2O_4$ composite photocatalyst combined photocatalysis and Fenton process for the better degradation efficiency of MO, bisphenol A and Escherichia coli. The H_2O_2 produced by Ag_3PO_4 could be catalytically decomposed into $^{\cdot}O_2^-$ and $^{\cdot}OH$ radicals by the $NiFe_2O_4$ nanoparticles decorated on the surface of Ag_3PO_4 via a photo-Fenton process ($Fe^{3+} + e^-$ (produced by $NiFe_2O_4$) $\rightarrow Fe^{2+}$; $Fe(OH)^{2+} + hv \rightarrow Fe^{2+} + {}^{\cdot}OH$; $Fe^{2+} + H_2O_2 \rightarrow Fe^{3+} + {}^{\cdot}OH + OH^-$; $Fe^{3+} + H_2O_2 \rightarrow Fe^{2+} + {}^{\cdot}OOH + H^+$). The main active specials in the photocatalysis process of this composite are demonstrated to be the h^+ (produced by Ag_3PO_4), $^{\cdot}O_2^-$ and $^{\cdot}OH$ radicals, and it is reasonable to conjecture that the enhanced photocatalytic activities are attributed to the conversion of H_2O_2 (produced by Ag_3PO_4) by $NiFe_2O_4$ through a photo-Fenton reaction. Combining photocatalysis with adsorption-desorption also is an interesting research direction. Generally, adsorption is a spontaneous process, while desorption usually need chemical or energy input. Using light as the energy source seems to be an ideal choice because it is finely tunable with high spatial and temporal accuracy, no transport limitations, available everywhere, no by-product, and non-invasive to the environment on demand. For example, recently, Xu et al. [213] prepared UIO-66-NH_2/Ag_3PO_4 nanoparticle composites for the adsorption of sulfamethoxazole (SMX). The authors declared that the light-sensitive Ag_3PO_4 nanoparticles of the composites is benefit for the desorption of SMX due to the transformation from Ag^+ to Ag^0. Accordingly, 200 mg/g SMX could be adsorbed by UIO-66-NH_2/Ag_3PO_4 composites, and 134/146 mg/g SMX can be desorbed. This work opened new opportunities for adsorption-desorption of targeted organic materials using visible light. However, up to now, discussion of

deposition of Ag_3PO_4 is really rare, which need researchers pay more attention in this field.

9. Conclusions and outlook

As a photocatalyst, silver phosphate has gained tremendous attention ever since its photocatalysis application was discovered back in 2010. Without doubt, it is one of the most promising photocatalyst even though some challenges still need to be conquered for industrialization and commercialization. In this regard, it is necessary to make a comprehensive understanding of the deep mechanism of its remarkable photocatalytic performance as well as the shortcoming while using it as photocatalyst in real-world situation. This review has discussed and summarized the recent progress in the field where Ag_3PO_4 was used as photocatalysts as well as some novel photoreactors for better photocatalytic activity. We briefly summarized the fundamental understanding of Ag_3PO_4 as photocatalyst by using computational techniques, and the difference of synthesis methods for fabricating terrific Ag_3PO_4 photocatalyst was also discussed. The obstacles that hinder its practical applications and the solutions to remove these obstacles were also presented in this review. Metal deposition could effectively suppress the photocorrosion phenomenon of Ag_3PO_4, thereby improving its photocatalytic activity, and protect it from dissolution in aqueous solution. By combining it with other materials, the composites could easily break the limitation such as limited light absorption range and high recombination rate of photogenerated charge carriers for a single component. Doping is also a feasible way to remove some obstacles that hinder the practical application of Ag_3PO_4. It could modify the surface structure, adjust the band gap energy, and influence the kinetic state of photoexcited charge carriers of Ag_3PO_4. Through subtly designing the synthetic process, we could achieve both elements doping and morphology control at the same time. However, it should be noted that not all elements doping are thermodynamically feasible. We need to put more efforts to study the feasibility of specific element doping, and the position of the dopant atoms in the lattice of host material. Excessive doping concentration could act as recombination centers, which should not be ignored. The development of photoreactors are another vital aspect for the practical application of photocatalysis. Never forget that we need highly efficient photoreactors which gear to actual circumstances to achieve the goal of practical application. In addition, the following items should be also addressed prior to practical application.

1) The mechanism of Ag_3PO_4 photocorrosion should be in-depth studied. Researchers demonstrated that metallic Ag could appear in both the synthesis process and photocatalysis process. Appropriate metallic Ag loading is conducive to its photocatalytic activity and stability. However, few researchers have discussed the exact amount of silver dissolving out from the lattice of Ag_3PO_4 in photocatalysis process. A quantizable Ag^0 generated by photocorrosion is favorable for the evaluation of modification effect. Extensive agglomeration of Ag nanoparticles would decrease the adsorption rate and capacity of Ag_3PO_4. Besides, the loading position of Ag on the surface of Ag_3PO_4 was rarely studied. Non-uniform diameters Ag nanoparticles randomly loading is undesirable for scientific studies. These two aspects are important for the further enhancement of photocatalytic performance of Ag_3PO_4.
2) The control of morphology, particle diameter, and surface states is important for the enhancement of photocatalytic performance of Ag_3PO_4-based materials. A short distance of the charges transferred from core to surface is beneficial to the decreases in the recombination of carriers. Besides, the surface of photocatalysts is the place where photocatalytic reactions occur. Different morphology, particle diameters, and surface states show different photodegradation capability towards pollutants. The relationship of these three factors needs to be further elaborated. In addition, synthesis methods have great influence on these factors. Thus, developing simple and green methods are needed to meet the requirements of practical application in the future.
3) Design of small amount Ag_3PO_4 loaded hybrid composite is an important subject for the practical application of Ag_3PO_4 owing to the high cost of pure Ag_3PO_4. However, there is a big controversy in distinguishing whether it is type II heterojunction or Z-scheme-like photocatalytic mechanism while the band gap of the two semiconductors are staggered. Thus, we need to develop a clear and direct technology to distinguish these two photocatalytic mechanisms. Besides, barely no researchers have studied the combination of doped Ag_3PO_4 with other semiconductor materials for the enhancement of photocatalytic performance, which we hope that some researchers would put strength to study this aspect in the future. Furthermore, theoretical simulation is a powerful technique for the design of photocatalyst, which should be abundantly using in the design stage. To experimentally prove the designed photocatalysts available is a low efficiency “try-error” methodology. Using theoretical simulation could give us a clear view whether the designed photocatalyst is theoretically feasible, and guide us to select the proper parameters for the optimal photocatalytic performance.
4) In order to turn laboratory-scale academic research into full-scale practical application to efficiently utilize solar energy as well as environmental purification, development of efficient pilot-scale treatment system is indispensable to provide useful information for further large-scale application. In addition, characteristics of Ag_3PO_4-based photocatalysts should be taken into consideration in the design of suitable photoreactors. Besides, there are mainly two ways to use the photocatalysts in reactors, i.e., using nanosized powder-like photocatalysts and using immobilized photocatalysts. Generally, nanosized powder-like Ag_3PO_4 hybrid composite photocatalyst possess higher photocatalytic activity than the immobilized ones. However, the separation of the nanosized powder-like Ag_3PO_4 hybrid composite photocatalyst in dispersion system and recycling of it are difficult, which needs further efforts to balance the superior photocatalytic activity (smaller particle size usually means higher photocatalytic activity) and recycling efficiency. We believe that an immobilized Ag_3PO_4-based photocatalyst with high photostability and photocatalytic activity is a feasible way for practical application, which should researchers put more strength in this aspect. Besides, although some researchers have studied coupling Ag_3PO_4 with some recyclable support materials such as aerogels, magnetic materials, small balls, and membranes, further efforts to develop recyclable Ag_3PO_4 based composite photocatalysts with excellent photocatalytic performance could not be ignored. Moreover, the rejuvenation of Ag_3PO_4-based photocatalyst is of great importance for the practical application. We expect researchers could pay more attention to this aspect, and hopefully designed a self-rejuvenated Ag_3PO_4-based hybrid composite to solve the photocorrosion problem.
5) To date, most studies have only tested the photocatalytic performance of Ag_3PO_4 under ideal conditions and focused on the degradation of single pollutant such as MO, Rh B, and phenol. However, in real-world situation, the circumstance of aqueous solution is much more complicated. Researchers should put more energy to discuss the outcomes while using modified Ag_3PO_4 photocatalysts to deal with the pollutants in real wastewater. The combination of physical, chemical, and microbiological means with photocatalytic treatment are required to get a desirable level of water quality.
6) Other than the aforementioned aspect, health concern of using Ag_3PO_4 as a photocatalyst should also put into consideration. With the using of Ag_3PO_4 as a photocatalyst, it is inevitable released some of it into the environment after the photocatalytic process. In consideration of its anti-bacterial property, the risk of leak of Ag_3PO_4 in environment to flora, fauna and human being health need to be carefully assessed. However, adverse effects of released Ag_3PO_4 in

the environment are still unknown. To the best of our knowledge, no research articles have been reported in this subject, and we hope some researchers could pay attention to this problem of Ag_3PO_4 in the future.

Acknowledgements

The study is financially supported by the Program for the National Natural Science Foundation of China (51521006, 5150817, 51779089, 51709101, and 51508177) and the Program for Changjiang Scholars and Innovative Research Team in University (IRT-13R17).

References

[1] P. Xu, G.M. Zeng, D.L. Huang, C.L. Feng, S. Hu, M.H. Zhao, C. Lai, Z. Wei, C. Huang, G.X. Xie, Use of iron oxide nanomaterials in wastewater treatment: a review, Sci. Total Environ. 424 (2012) 1–10.
[2] X. Tan, Y. Liu, G. Zeng, X. Wang, X. Hu, Y. Gu, Z. Yang, Application of biochar for the removal of pollutants from aqueous solutions, Chemosphere 125 (2015) 70–85.
[3] F. Long, J.L. Gong, G.M. Zeng, L. Chen, X.Y. Wang, J.H. Deng, Q.Y. Niu, H.Y. Zhang, X.R. Zhang, Removal of phosphate from aqueous solution by magnetic Fe–Zr binary oxide, Chem. Eng. J. 171 (2011) 448–455.
[4] P. Xu, G.M. Zeng, D.L. Huang, C. Lai, M.H. Zhao, Z. Wei, N.J. Li, C. Huang, G.X. Xie, Adsorption of Pb(II) by iron oxide nanoparticles immobilized Phanerochaete chrysosporium : equilibrium, kinetic, thermodynamic and mechanisms analysis, Chem. Eng. J. 203 (2012) 423–431.
[5] W.W. Tang, G.M. Zeng, J.L. Gong, J. Liang, P. Xu, C. Zhang, B.B. Huang, Impact of humic/fulvic acid on the removal of heavy metals from aqueous solutions using nanomaterials: a review, Sci. Total Environ. 468–469 (2014) 1014–1027.
[6] M. Chen, P. Xu, G. Zeng, C. Yang, D. Huang, J. Zhang, Bioremediation of soils contaminated with polycyclic aromatic hydrocarbons, petroleum, pesticides, chlorophenols and heavy metals by composting: applications, microbes and future research needs, Biotechnol. Adv. 33 (2015) 745–755.
[7] J. Liang, Z. Yang, L. Tang, G. Zeng, M. Yu, X. Li, H. Wu, Y. Qian, X. Li, Y. Luo, Changes in heavy metal mobility and availability from contaminated wetland soil remediated with combined biochar-compost, Chemosphere 181 (2017) 281.
[8] H. Wu, C. Lai, G. Zeng, J. Liang, J. Chen, J. Xu, J. Dai, X. Li, J. Liu, M. Chen, The interactions of composting and biochar and their implications for soil amendment and pollution remediation: a review, Crit. Rev. Biotechnol. 37 (2017) 754–764.
[9] Y. Zhang, G.M. Zeng, L. Tang, J. Chen, Y. Zhu, X.X. He, Y. He, Electrochemical sensor based on electrodeposited graphene-Au modified electrode and nanoAu carrier amplified signal strategy for attomolar mercury detection, Anal. Chem. 87 (2015) 989–996.
[10] J. Wan, G. Zeng, D. Huang, L. Hu, P. Xu, C. Huang, R. Deng, W. Xue, C. Lai, C. Zhou, Rhamnolipid stabilized nano-chlorapatite: Synthesis and enhancement effect on Pb-and Cd-immobilization in polluted sediment, J. Hazard. Mater. 343 (2017).
[11] X. Ren, G. Zeng, L. Tang, J. Wang, J. Wan, Y. Liu, J. Yu, H. Yi, S. Ye, R. Deng, Sorption, transport and biodegradation - An insight into bioavailability of persistent organic pollutants in soil, Sci. Total Environ. 610–611 (2017) 1154–1163.
[12] Y. Lin, S. Wu, X. Li, X. Wu, C. Yang, G. Zeng, Y. Peng, Q. Zhou, L. Lu, Microstructure and performance of Z-scheme photocatalyst of silver phosphate modified by MWCNTs and Cr-doped SrTiO3 for malachite green degradation, Appl. Catal. B 227 (2018) 557–570.
[13] F. Chen, Q. Yang, Y. Zhong, H. An, J. Zhao, T. Xie, Q. Xu, X. Li, D. Wang, G. Zeng, Photo-reduction of bromate in drinking water by metallic Ag and reduced graphene oxide (RGO) jointly modified BiVO4 under visible light irradiation, Water Res. 101 (2016) 555–563.
[14] F. Chen, Q. Yang, X. Li, G. Zeng, D. Wang, C. Niu, J. Zhao, H. An, T. Xie, Y. Deng, Hierarchical assembly of graphene-bridged Ag 3 PO 4/Ag/BiVO 4 (040) Z-scheme photocatalyst: An efficient, sustainable and heterogeneous catalyst with enhanced visible-light photoactivity towards tetracycline degradation under visible light irradiation, Appl. Catal. B 200 (2017) 330–342.
[15] M. Cheng, G. Zeng, D. Huang, L. Cui, P. Xu, C. Zhang, Y. Liu, Hydroxyl radicals based advanced oxidation processes (AOPs) for remediation of soils contaminated with organic compounds: a review, Chem. Eng. J. 284 (2016) 582–598.
[16] W. Dong, D. Wang, H. Wang, M. Li, F. Chen, F. Jia, Q. Yang, X. Li, X. Yuan, J. Gong, Facile synthesis of In2S3/UiO-66 composite with enhanced adsorption performance and photocatalytic activity for the removal of tetracycline under visible light irradiation, J. Colloid Interface Sci. 535 (2019) 444–457.
[17] D. Wang, F. Jia, H. Wang, F. Chen, Y. Fang, W. Dong, G. Zeng, X. Li, Q. Yang, X. Yuan, efficient adsorption and photocatalytic degradation of tetracycline by Fe-based MOFs, J. Colloid Interface Sci. 519 (2018) 273.
[18] C. Zhou, C. Lai, D. Huang, G. Zeng, C. Zhang, M. Cheng, L. Hu, J. Wan, W. Xiong, M. Wen, Highly porous carbon nitride by supramolecular preassembly of monomers for photocatalytic removal of sulfamethazine under visible light driven, Appl. Catal. B 220 (2017).
[19] C. Zhou, C. Lai, P. Xu, G. Zeng, D. Huang, C. Zhang, M. Cheng, L. Hu, J. Wan, Y. Liu, In situ grown AgI/$Bi_{12}O_{17}Cl_2$ heterojunction photocatalysts for visible light degradation of sulfamethazine: efficiency, pathway and mechanism, ACS Sustainable Chem. Eng. (2018).
[20] F. Chen, Q. Yang, X. Li, D. Wang, Y. Zhong, J. Zhao, Y. Deng, C. Niu, G. Zeng, Promotion of $ZnSn(OH)_6$ photoactivity by constructing heterojunction with Ag@Ag_3PO_4 nanoparticles: visible light elimination of single or multiple dyes, Catal. Commun. 84 (2016) 137–141.
[21] F. Chen, Q. Yang, J. Sun, F. Yao, S. Wang, Y. Wang, X. Wang, X. Li, C. Niu, D. Wang, Enhanced photocatalytic degradation of tetracycline by AgI/BiVO4 heterojunction under visible-light irradiation: mineralization efficiency and mechanism, ACS Appl. Mater. Interfaces 8 (2016) 32887.
[22] H. Dong, G. Zeng, L. Tang, C. Fan, C. Zhang, X. He, Y. He, An overview on limitations of TiO2-based particles for photocatalytic degradation of organic pollutants and the corresponding countermeasures, Water Res. 79 (2015) 128–146.
[23] H. Tong, S. Ouyang, Y. Bi, N. Umezawa, M. Oshikiri, J. Ye, Nano-photocatalytic materials: possibilities and challenges, Adv. Mater. 24 (2012) 229.
[24] Y. Yang, C. Zhang, C. Lai, G. Zeng, D. Huang, M. Cheng, J. Wang, F. Chen, C. Zhou, W. Xiong, BiOX (X = Cl, Br, I) photocatalytic nanomaterials: applications for fuels and environmental management, Adv. Colloid Interface Sci. (2018).
[25] A. Fujishima, K. Honda, Electrochemical photolysis of water at a semiconductor electrode, Nature 238 (1972) 37–38.
[26] X. Chen, S.S. Mao, Titanium dioxide nanomaterials: synthesis, properties, modifications, and applications, Chem. Rev. 107 (2007) 2891.
[27] Stefano Livraghi, M.C. Paganini, Elio Giamello, Annabella Selloni, C.D. Valentin, G. Pacchioni, Origin of photoactivity of nitrogen-doped titanium dioxide under visible light, J. Am. Chem. Soc. 128 (2006) 15666–15671.
[28] R. Leary, A. Westwood, Carbonaceous nanomaterials for the enhancement of TiO photocatalysis, Carbon 49 (2011) 741–772.
[29] T. Umebayashi, T. Yamaki, H. Itoh, K. Asai, Band gap narrowing of titanium dioxide by sulfur doping, Appl. Phys. Lett. 81 (2002) 454–456.
[30] D. Peichang, H. Jiezhen, W. Haizeng, S. Baowei, Hydrothermal preparation and comparative study of halogen-doping TiO2 photocatalysts, J. Adv. Oxidat. Technol. 13 (2010) 200-205(206).
[31] D. Li, H. Haneda, S. Hishita, N. Ohashi, N.K. Labhsetwar, Fluorine-doped TiO2 powders prepared by spray pyrolysis and their improved photocatalytic activity for decomposition of gas-phase acetaldehyde, J. Fluorine Chem. 126 (2005) 69–77.
[32] T. Umebayashi, T. Yamaki, H. Itoh, K. Asai, Analysis of electronic structures of 3d transition metal-doped TiO 2 based on band calculations, J. Phys. Chem. Solids 63 (2002) 1909–1920.
[33] M. Salmi, N. Tkachenko, R.J. Lamminmäki, S. Karvinen, V. Vehmanen, H. Lemmetyinen, Femtosecond to nanosecond spectroscopy of transition metal-doped TiO2 particles, J. Photochem. Photobiol., A 175 (2005) 8–14.
[34] Z. Zheng, B. Huang, X. Qin, X. Zhang, Y. Dai, M.H. Whangbo, Facile synthesis of visible-light plasmonic photocatalysts M@TiO (M = Au, Pt, Ag) and evaluation of their photocatalytic oxidation of benzene to phenol, J. Mater. Chem. 21 (2011) 9079–9087.
[35] Z. Hao, L. Xiaojun, L. Yueming, W. Ying, L. Jinghong, P25-graphene composite as a high performance photocatalyst, ACS Nano 4 (2010) 380–386.
[36] W. Graeme, S. Brian, P.V. Kamat, TiO2-graphene nanocomposites. UV-assisted photocatalytic reduction of graphene oxide, ACS Nano 2 (2008) 1487.
[37] L. Joon Seok, Y. Kyeong Hwan, P.C. Beum, Highly photoactive, low bandgap TiO2 nanoparticles wrapped by graphene, Adv. Mater. 24 (2012) 1133–1133.
[38] Y. Bessekhouad, D. Robert, J.V. Weber, Bi2S3/TiO2 and CdS/TiO2 heterojunctions as an available configuration for photocatalytic degradation of organic pollutant, J. Photochem. Photobiol., A 163 (2004) 569–580.
[39] A. Kongkanand, K. Tvrdy, K. Takechi, M. Kuno, P.V. Kamat, Quantum dot solar cells. Tuning photoresponse through size and shape control of CdSe-TiO2 architecture, J. Am. Chem. Soc. 130 (2008) 4007–4015.
[40] Zhenfeng Bian, J. Zhu, Shaohua Wang, Y. Cao, A. Xufang Qian, Hexing Li, Self-assembly of active Bi2O3/TiO2 visible photocatalyst with ordered mesoporous structure and highly crystallized anatase, J. Phys. Chem. C 112 (2008) 6258–6262.
[41] Y.T. Kwon, Y.S. Kang, I.L. Wan, G.J. Choi, Y.R. Do, Photocatalytic behavior of WO3-loaded TiO 2 in an oxidation reaction, J. Catal. 191 (2000) 192–199.
[42] L. Yang, S. Luo, Y. Li, Y. Xiao, Q. Kang, Q. Cai, High efficient photocatalytic degradation of p-nitrophenol on a unique Cu2O/TiO2 p-n heterojunction network catalyst, Environ. Sci. Technol. 44 (2010) 7641–7646.
[43] K. Vinodgopal, P.V. Kamat, Enhanced rates of photocatalytic degradation of an azo dye using SnO2/TiO2 coupled semiconductor thin films, Environ. Sci. Technol. 29 (1995) 841–845.
[44] K.S. Girish, D.L. Gomathi, Review on modified TiO2 photocatalysis under UV/visible light: selected results and related mechanisms on interfacial charge carrier transfer dynamics, J. Phys. Chem. A 115 (2011) 13211–13241.
[45] J. Thomas, K.P. Kumar, K.R. Chitra, Synthesis of Ag doped nano TiO2 as efficient solar photocatalyst for the degradation of endosulfan, J. Comput. Theor. Nanosci. 4 (2011) 108–114.
[46] W. Jin, T. De Nyago, J.P. Lewis, H. Zhanglian, M. Ayyakkannu, Z. Mingjia, L. Ming, W. Nianqiang, Origin of photocatalytic activity of nitrogen-doped TiO2 nanobelts, J. Am. Chem. Soc. 131 (2009) 12290–12297.
[47] L.G. Devi, R. Kavitha, A review on non metal ion doped titania for the photocatalytic degradation of organic pollutants under UV/solar light: role of photogenerated charge carrier dynamics in enhancing the activity, Appl. Catal. B 140–141 (2013) 559–587.
[48] M.A. Butler, Photoelectrolysis and physical properties of the semiconducting electrode WO/sub 2, J. Appl. Phys. 48 (1977) 1914–1920.
[49] T.W. Kim, K.S. Choi, Nanoporous BiVO4 photoanodes with dual-layer oxygen evolution catalysts for solar water splitting, Cheminform 45 (2014) 990–994.
[50] Y. Yang, Z. Zeng, Z. Chen, D. Huang, G. Zeng, X. Rong, L. Cui, C. Zhou, G. Hai,

W. Xue, Construction of iodine vacancy-rich BiOI/Ag@AgI Z-scheme heterojunction photocatalysts for visible-light-driven tetracycline degradation: transformation pathways and mechanism insight, Chem. Eng. J. (2018) S1385894718309069.
[51] Y. Wang, X. Wang, M. Antonietti, Polymeric graphitic carbon nitride as a heterogeneous organocatalyst: from photochemistry to multipurpose catalysis to sustainable chemistry, Angew. Chem. Int. Ed. 51 (2012) 68–89.
[52] Z. Yi, J. Ye, N. Kikugawa, T. Kako, S. Ouyang, H. Stuartwilliams, H. Yang, J. Cao, W. Luo, Z. Li, An orthophosphate semiconductor with photooxidation properties under visible-light irradiation, Nat. Mater. 9 (2010) 559–564.
[53] P. Dong, Y. Hao, P. Gao, E. Cui, Q. Zhang, Synthesis and photocatalytic activity of Ag3PO4 triangular prism, J. Nanomater. 2015 (2015) 221–236.
[54] T.L.R. Hewer, B.C. Machado, R.S. Freire, R. Guardani, Ag3PO4 sunlight-induced photocatalyst for degradation of phenol, RSC Adv. 4 (2014) 34674–34680.
[55] K. Baďurová, O. Monfort, L. Satrapinskyy, E. Dworniczek, G. Gościniak, G. Plesch, Photocatalytic activity of Ag 3 PO 4 and some of its composites under non-filtered and UV-filtered solar-like radiation, Ceram. Int. 43 (2016) 3706.
[56] U. Sulaeman, I.R. Nisa, A. Riapanitra, P. Iswanto, S. Yin, T. Sato, The highly active photocatalyst of silver orthophosphate under visible light irradiation for phenol oxidation, Adv. Mater. Res. 896 (2014) 141–144.
[57] K. Hatakeyama, M. Okuda, T. Kuki, T. Esaka, Removal of dissolved humic acid from water by photocatalytic oxidation using a silver orthophosphate semiconductor, Mater. Res. Bull. 47 (2012) 4478–4482.
[58] H. Huang, Y. Feng, J. Zhou, G. Li, K. Dai, Visible light photocatalytic reduction of Cr(VI) on AgPOnanoparticles, Desalin. Water Treat. 51 (2013) 7236–7240.
[59] P. Amornpitoksuk, K. Intarasuwan, S. Suwanboon, J. Baltrusaitis, Effect of phosphate salts (Na3PO4, Na2HPO4, and NaH2PO4) on Ag3PO4 morphology for photocatalytic dye degradation under visible light and toxicity of the degraded dye products, Ind. Eng. Chem. Res. 52 (2013) 17369–17375.
[60] W. Kai, J. Xu, H. Xia, L. Na, M. Chen, T. Fei, Y. Zhu, W. Yao, Highly efficient photodegradation of RhB–MO mixture dye wastewater by Ag3PO4 dodecahedrons under acidic condition, J. Mol. Catal. A: Chem. 393 (2014) 302–308.
[61] J. Zhang, K. Yu, L. Lou, C. Ma, L. Liao, M. Yi, S. Liu, Visible-light photocatalytic activity of Ag3PO4 with different particle sizes for the degradation of bisphenol A in water, Disaster Adv. 6 (2013) 109–117.
[62] Z. Frontistis, M. Antonopoulou, A. Petala, D. Venieri, I. Konstantinou, D.I. Kondarides, D. Mantzavinos, Photodegradation of ethyl paraben using simulated solar radiation and Ag3PO4 photocatalyst, J. Hazard. Mater. 323 (2017) 478.
[63] J. Gou, Q. Ma, Y. Cui, X. Deng, H. Zhang, X. Cheng, X. Li, M. Xie, Q. Cheng, H. Liu, Visible light photocatalytic removal performance and mechanism of diclofenac degradation by Ag 3 PO 4 sub-microcrystals through response surface methodology, J. Ind. Eng. Chem. 49 (2017) 112–121.
[64] Y. Liu, G. Zhu, J. Yang, A. Yuan, X. Shen, Peroxidase-like catalytic activity of Ag3PO4 nanocrystals prepared by a colloidal route, PLoS One 9 (2014) e109158.
[65] F. Teng, Z. Liu, A. Zhang, M. Li, Photocatalytic performances of Ag3PO4 polypods for degradation of dye pollutant under natural indoor weak light irradiation, Environ. Sci. Technol. 49 (2015) 9489–9494.
[66] Y. Chang, K. Yu, C. Zhang, R. Li, P. Zhao, L.L. Lou, S. Liu, Three-dimensionally ordered macroporous WO 3 supported Ag 3 PO 4 with enhanced photocatalytic activity and durability, Appl. Catal. B 176–177 (2015) 363–373.
[67] H. Fu, W. Yao, L. Zhang, Y. Zhu, The enhanced photoactivity of nanosized Bi2WO6 catalyst for the degradation of 4-chlorophenol, Mater. Res. Bull. 43 (2008) 2617–2625.
[68] J. Tang, Z. Zou, J. Ye, Photocatalytic decomposition of organic contaminants by Bi 2 WO 6 under visible light irradiation, Catal. Lett. 92 (2004) 53–56.
[69] A. Kudo, S. Hijii, H_2 or O_2 evolution from aqueous solutions on layered oxide photocatalysts consisting of Bi^{3+} with $6s^2$ configuration and d^0 transition metal ions, Chem. Lett. 1999 (1999) 1103–1104.
[70] S. Zhang, X. Gu, Y. Zhao, Y. Qiang, Effect of annealing temperature and time on structure, morphology and visible-light photocatalytic activities Ag3PO4 microparticles, Mater. Sci. Eng., B 201 (2015) 57–65.
[71] X. Chen, Y. Dai, X. Wang, Methods and mechanism for improvement of photocatalytic activity and stability of Ag3PO4: a review, J. Alloy Compd. 649 (2015) 910–932.
[72] N. Umezawa, O. Shuxin, J. Ye, Theoretical study of high photocatalytic performance of Ag3PO4, Phys. Rev. B 83 (2011) 287–292.
[73] X. Ma, B. Lu, D. Li, R. Shi, C. Pan, Y. Zhu, Origin of photocatalytic activation of silver orthophosphate from first-principles, J. Phys. Chem. C 115 (2011) 4680–4687.
[74] Y. Bi, H. Yu, B. Jin, C. Feng, Z. Jiao, G. Lu, Facile synthesis of porous Ag3PO4 photocatalysts with high self-stability and activity, RSC Adv. 6 (2016) 56166–56169.
[75] J. Wang, F. Teng, M. Chen, J. Xu, Y. Song, X. Zhou, Facile synthesis of novel Ag3PO4 tetrapods and the 110 facets-dominated photocatalytic activity, CrystEngComm 15 (2012) 39–42.
[76] A. Khan, M. Qamar, M. Muneer, Synthesis of highly active visible-light-driven colloidal silver orthophosphate, Chem. Phys. Lett. 519 (2012) 54–58.
[77] Z. Jiao, Y. Zhang, H. Yu, G. Lu, J. Ye, Y. Bi, Concave trisoctahedral Ag3PO4 microcrystals with high-index facets and enhanced photocatalytic properties, Chem. Commun. 49 (2013) 636–638.
[78] Y. Bi, H. Hu, S. Ouyang, G. Lu, J. Cao, J. Ye, ChemInform abstract: photocatalytic and photoelectric properties of cubic Ag3PO4 sub-microcrystals with sharp corners and edges, Cheminform 48 (2012) 3748–3750.
[79] Y. Bi, S. Ouyang, N. Umezawa, J. Cao, J. Ye, Facet effect of single-crystalline Ag3PO4 sub-microcrystals on photocatalytic properties, J. Am. Chem. Soc. 133 (2011) 6490–6492.
[80] J. Wan, L. Sun, J. Fan, E. Liu, X. Hu, C. Tang, Y. Yin, Facile synthesis of porous Ag3PO4 nanotubes for enhanced photocatalytic activity under visible light, Appl. Surf. Sci. 355 (2015) 615–622.
[81] X. Guan, J. Shi, L. Guo, Ag3PO4 photocatalyst: hydrothermal preparation and enhanced O2 evolution under visible-light irradiation, Int. J. Hydrogen Energy 38 (2013) 11870–11877.
[82] H.H. Ou, S.L. Lo, Review of titania nanotubes synthesized via the hydrothermal treatment: fabrication, modification, and application, Sep. Purif. Technol. 58 (2007) 179–191.
[83] L. An-Hui, E.L. Salabas, S. Ferdi, Magnetic nanoparticles: synthesis, protection, functionalization, and application, Angew. Chem. Int. Ed. 46 (2010) 1222–1244.
[84] S. Weidong, S. Shuyan, Z. Hongjie, Hydrothermal synthetic strategies of inorganic semiconducting nanostructures, Chem. Soc. Rev. 42 (2013) 5714–5743.
[85] Z. Chen, W. Wang, Z. Zhang, X. Fang, High-efficiency visible-light-driven Ag3PO4/AgI photocatalysts: Z-scheme photocatalytic mechanism for their enhanced photocatalytic activity, J. Phys. Chem. C 117 (2013) 19346–19352.
[86] X. Yao, Z. Huang, Z. Zhang, X. Zhang, R. Wen, Y. Liu, M. Fang, X. Wu, Controlled synthesis and photocatalytic properties of rhombic dodecahedral Ag3PO4 with high surface energy, Appl. Surf. Sci. 389 (2016) 56–66.
[87] X. Cui, Y.F. Zheng, H. Zhou, H.Y. Yin, X.C. Song, The effect of synthesis temperature on the morphologies and visible light photocatalytic performance of Ag3PO4, J. Taiwan Inst. Chem. Eng. 60 (2016) 328–334.
[88] Y. Ma, Q. Kuang, Z. Jiang, Z. Xie, R. Huang, L. Zheng, Synthesis of trisoctahedral gold nanocrystals with exposed high-index facets by a facile chemical method, Angew. Chem. 120 (2008) 9033–9036.
[89] D.J. Martin, N. Umezawa, X. Chen, J. Ye, J. Tang, Facet engineered Ag3PO4 for efficient water photooxidation, Energy Environ. Sci. 6 (2013) 3380–3386.
[90] M.S. Hsieh, H.J. Su, P.L. Hsieh, Y.W. Chiang, M.H. Huang, Synthesis of Ag3PO4 crystals with tunable shapes for facet-dependent optical property, photocatalytic activity and electrical conductivity examinations, ACS Appl. Mater. Interfaces (2017).
[91] S. Kim, Y. Wang, M. Zhu, M. Fujitsuka, T. Majima, Facet effects of Ag3PO4 on charge-carrier dynamics: trade-off between photocatalytic activity and charge-carrier lifetime, Chemistry 24 (2018) 14928–14932.
[92] U. Sulaeman, D. Hermawan, R. Andreas, A.Z. Abdullah, S. Yin, Native defects in silver orthophosphate and their effects on photocatalytic activity under visible light irradiation, Appl. Surf. Sci. 428 (2018).
[93] W. Hou, S.B. Cronin, A review of surface plasmon resonance-enhanced photocatalysis, Adv. Funct. Mater. 23 (2013) 1612–1619.
[94] D. Ding, K. Liu, S. He, C. Gao, Y. Yin, Ligand-exchange assisted formation of Au/TiO2 Schottky contact for visible-light photocatalysis, Nano Lett. 14 (2014) 6731.
[95] S. Bai, J. Jiang, Q. Zhang, Y. Xiong, Steering charge kinetics in photocatalysis: intersection of materials syntheses, characterization techniques and theoretical simulations, Chem. Soc. Rev. 46 (2015) 2893–2939.
[96] Y. Qu, X. Duan, Progress, challenge and perspective of heterogeneous photocatalysts, Chem. Soc. Rev. 42 (2013) 2568–2580.
[97] Y. Liu, L. Fang, H. Lu, L. Liu, H. Wang, C. Hu, Highly efficient and stable Ag/Ag3PO4 plasmonic photocatalyst in visible light, Catal. Commun. 17 (2012) 200–204.
[98] T. Wei, X. Li, Q. Zhao, J. Zhao, D. Zhang, In situ capture of active species and oxidation mechanism of RhB and MB dyes over sunlight-driven Ag/Ag3PO4 plasmonic nanocatalyst, Appl. Catal. B 125 (2012) 538–545.
[99] J. Wan, E. Liu, J. Fan, X. Hu, L. Sun, C. Tang, Y. Yin, H. Li, Y. Hu, In-situ synthesis of plasmonic Ag/Ag 3 PO 4 tetrahedron with exposed 111 facets for high visible-light photocatalytic activity and stability, Ceram. Int. 41 (2015) 6933–6940.
[100] S.S. Patil, D.R. Patil, S.K. Apte, M.V. Kulkarni, J.D. Ambekar, C.J. Park, S.W. Gosavi, S.S. Kolekar, B.B. Kale, Confinement of Ag 3 PO 4 nanoparticles supported by surface plasmon resonance of Ag in glass: Efficient nanoscale photocatalyst for solar H 2 production from waste H 2 S, Appl. Catal. B 190 (2016) 75–84.
[101] T. Yan, H. Zhang, Y. Liu, W. Guan, J. Long, W. Li, J. You, Fabrication of robust M/Ag3PO4 (M = Pt, Pd, Au) Schottky-type heterostructures for improved visible-light photocatalysis, RSC Adv. 4 (2014) 37220–37230.
[102] F.R. Wang, J.D. Wang, H.P. Sun, J.K. Liu, X.H. Yang, Plasmon-enhanced instantaneous photocatalytic activity of Au@Ag3PO4 heterostructure targeted at emergency treatment of environmental pollution, J. Mater. Sci. 52 (2016) 2495–2510.
[103] Z. Liu, Y. Liu, P. Xu, Z. Ma, J. Wang, H. Yuan, Rational design of wide spectral-responsive heterostructures of Au nanorod coupled Ag3PO4 with enhanced photocatalytic performance, ACS Appl. Mater. Interfaces 9 (2017) 20620.
[104] Y. Cao, Z. Wu, J. Ni, W.A. Bhutto, L. Jing, S. Li, H.J.K. Kai, Type-I I core/shell nanowire heterostructures and their photovoltaic applications, Nano-Micro Lett. 4 (2012) 135–141.
[105] V.O. Ozcelik, J.G. Azadani, C. Yang, S.J. Koester, T. Low, Band alignment of 2D semiconductors for designing heterostructures with momentum space matching, Phys. Rev. B 94 (2016) 035125.
[106] W. Yao, B. Zhang, C. Huang, C. Ma, X. Song, Q. Xu, Synthesis and characterization of high efficiency and stable Ag3PO4/TiO2 visible light photocatalyst for the degradation of methylene blue and rhodamine B solutions, J. Mater. Chem. 22 (2012) 4050–4055.
[107] T.S. Natarajan, K.R. Thampi, R.J. Tayade, Visible light driven redox-mediator-free dual semiconductor photocatalytic systems for pollutant degradation and the ambiguity in applying Z-scheme concept, Appl. Catal. B Environ. (2018) S0926337318300225.
[108] L. Wang, Y. Chai, J. Ren, J. Ding, Q. Liu, W.L. Dai, Ag3PO4 nanoparticles loaded on 3D flower-like spherical MoS2: a highly efficient hierarchical heterojunction

photocatalyst, Dalton Trans. 44 (2015) 14625–14634.
[109] Y. Song, Y. Lei, H. Xu, C. Wang, J. Yan, H. Zhao, Y. Xu, J. Xia, S. Yin, H. Li, Synthesis of few-layer MoS2 nanosheet-loaded Ag3PO4 for enhanced photocatalytic activity, Dalton Trans. 44 (2015) 3057.
[110] C. Zhu, L. Zhang, B. Jiang, J. Zheng, P. Hu, S. Li, M. Wu, W. Wu, Fabrication of Z-scheme Ag 3 PO 4/MoS 2 composites with enhanced photocatalytic activity and stability for organic pollutant degradation, Appl. Surf. Sci. 377 (2016) 99–108.
[111] X. Wang, K. Maeda, A. Thomas, K. Takanabe, G. Xin, J.M. Carlsson, K. Domen, M. Antonietti, A metal-free polymeric photocatalyst for hydrogen production from water under visible light, Nat. Mater. 8 (2009) 76–80.
[112] C. Pan, J. Xu, Y. Wang, D. Li, Y. Zhu, Dramatic activity of C3N4/BiPO4 photocatalyst with core/shell structure formed by self-assembly, Adv. Funct. Mater. 22 (2012) 1518–1524.
[113] S. Chen, Y. Hu, S. Meng, X. Fu, Study on the separation mechanisms of photogenerated electrons and holes for composite photocatalysts g-C3 N4-WO3, Appl. Catal. B Environ. 150–151 (2014) 564–573.
[114] Y. Yang, C. Zhang, D. Huang, G. Zeng, J. Huang, C. Lai, C. Zhou, W. Wang, H. Guo, W. Xue, R. Deng, M. Cheng, W. Xiong, Boron nitride quantum dots decorated ultrathin porous g-C3N4: Intensified exciton dissociation and charge transfer for promoting visible-light-driven molecular oxygen activation, Appl. Catal. B 245 (2019) 87–99.
[115] Y. He, L. Zhang, B. Teng, M. Fan, New application of Z-scheme Ag3PO4/g-C3N4 composite in converting CO2 to fuel, Environ. Sci. Technol. 49 (2015) 649–656.
[116] T. Xu, R. Zhu, J. Zhu, X. Liang, G. Zhu, Y. Liu, Y. Xu, H. He, Fullerene modification of Ag3PO4 for the visible-light-driven degradation of acid red 18, RSC Adv. 6 (2016).
[117] X. Yang, H. Cui, Y. Li, J. Qin, R. Zhang, H. Tang, Fabrication of Ag3PO4-graphene composites with highly efficient and stable visible light photocatalytic performance, ACS Catal. 3 (2013) 363–369.
[118] J.Y. Sun, X. Zhao, W.R.K. Illeperuma, O. Chaudhuri, K.H. Oh, D.J. Mooney, J.J. Vlassak, Z. Suo, Highly stretchable and tough hydrogels, Nature 489 (2012) 133–136.
[119] G. Panthi, S.J. Park, S.H. Chae, T.W. Kim, H.J. Chung, S.T. Hong, M. Park, H.Y. Kim, Immobilization of Ag 3 PO 4 nanoparticles on electrospun PAN nanofibers via surface oximation: Bifunctional composite membrane with enhanced photocatalytic and antimicrobial activities, J. Ind. Eng. Chem. (2016).
[120] L. Liu, L. Ding, Y. Liu, W. An, S. Lin, Y. Liang, W. Cui, A stable Ag3PO4 @PANI core@shell hybrid: enrichment photocatalytic degradation with π-π conjugation, Appl. Catal. B 201 (2017) 92–104.
[121] H. Yue, S. Huang, X. Zheng, F. Cao, T. Yu, G. Zhang, Z. Xiao, J.N. Liang, Y. Zhang, Synthesis of core-shell structured Ag3PO4@benzoxazine soft gel nanocomposites and their photocatalytic performance, RSC Adv. 6 (2016).
[122] S. Mosleh, M.R. Rahimi, M. Ghaedi, K. Dashtian, S. Hajati, S. Wang, Ag 3 PO 4/AgBr/Ag-HKUST-1-MOF composites as novel blue LED light active photocatalyst for enhanced degradation of ternary mixture of dyes in a rotating packed bed reactor, Chem. Eng. Process. Process Intensif. 114 (2017) 24–38.
[123] F.A. Sofi, K. Majid, O. Mehraj, The visible light driven copper based metal-organic-framework heterojunction:HKUST-1@Ag-Ag3 PO4 for plasmon enhanced visible light photocatalysis, J. Alloy. Compd. 737 (2018) 798–808.
[124] S. Mosleh, M.R. Rahimi, M. Ghaedi, K. Dashtian, Sonophotocatalytic degradation of trypan blue and vesuvine dyes in the presence of blue light active photocatalyst of Ag3 PO4/Bi2 S3 -HKUST-1-MOF: central composite optimization and synergistic effect study, Ultrason. Sonochem. 32 (2016) 387–397.
[125] J.L. Gong, B. Wang, G.M. Zeng, C.P. Yang, C.G. Niu, Q.Y. Niu, W.J. Zhou, Y. Liang, Removal of cationic dyes from aqueous solution using magnetic multi-wall carbon nanotube nanocomposite as adsorbent, J. Hazard. Mater. 164 (2009) 1517–1522.
[126] J.H. Deng, X.R. Zhang, G.M. Zeng, J.L. Gong, Q.Y. Niu, J. Liang, Simultaneous removal of Cd(II) and ionic dyes from aqueous solution using magnetic graphene oxide nanocomposite as an adsorbent, Chem. Eng. J. 226 (2013) 189–200.
[127] C. Zhang, C. Lai, G. Zeng, D. Huang, C. Yang, Y. Wang, Y. Zhou, M. Cheng, Efficacy of carbonaceous nanocomposites for sorbing ionizable antibiotic sulfamethazine from aqueous solution, Water Res. 95 (2016) 103.
[128] G. Li, Y. Li, H. Liu, Y. Guo, Y. Li, D. Zhu, Architecture of graphdiyne nanoscale films, Chem. Commun. 46 (2010) 3256–3258.
[129] M. Long, L. Tang, D. Wang, Y. Li, Z. Shuai, Electronic structure and carrier mobility in graphdiyne sheet and nanoribbons: theoretical predictions, ACS Nano 5 (2011) 2593–2600.
[130] Y. Tang, H. Yang, P. Yang, Investigation on the contact between graphdiyne and Cu (111) surface, Carbon 117 (2017) 246–251.
[131] Q. Peng, A.K. Dearden, J. Crean, L. Han, S. Liu, X. Wen, S. De, New materials graphyne, graphdiyne, graphone, and graphane: review of properties, synthesis, and application in nanotechnology, Nanotechnol. Sci. Appl. 7 (2014) 1–29.
[132] S. Guo, Y. Jiang, F. Wu, P. Yu, H. Liu, Y. Li, L. Mao, Graphdiyne-promoted highly efficient photocatalytic activity of graphdiyne/silver phosphate pickering emulsion under visible-light irradiation, ACS Appl. Mater. Interfaces (2018).
[133] R. Liu, Z. Zheng, J. Spurgeon, X. Yang, Enhanced photoelectrochemical water-splitting performance of semiconductors by surface passivation layers, Energy Environ. Sci. 7 (2014) 2504–2517.
[134] F. Chen, S. Li, Q. Chen, X. Zheng, P. Liu, S. Fang, 3D graphene aerogels-supported Ag and Ag@Ag3PO4 heterostructure for the efficient adsorption-photocatalysis capture of different dye pollutants in water, Mater. Res. Bull. 105 (2018) 334–341.
[135] T. Yan, J. Tian, W. Guan, Z. Qiao, W. Li, J. You, B. Huang, Ultra-low loading of Ag3PO4 on hierarchical In2S3 microspheres to improve the photocatalytic performance: the cocatalytic effect of Ag and Ag3PO4, Appl. Catal. B 202 (2017) 84–94.
[136] C. Zhang, K. Yu, Y. Feng, Y. Chang, T. Yang, Y. Xuan, D. Lei, L.L. Lou, S. Liu, Novel 3DOM-SrTiO 3/Ag/Ag 3 PO 4 ternary Z-scheme photocatalysts with remarkably improved activity and durability for contaminant degradation, Appl. Catal. B 210 (2017).
[137] X.Q. Liu, W.J. Chen, H. Jiang, Facile synthesis of Ag/Ag 3 PO 4/AMB composite with improved photocatalytic performance, Chem. Eng. J. 308 (2017) 889–896.
[138] W. Xiong, W. Dai, X. Hu, L. Yang, T. Wang, Y. Qin, X. Luo, J. Zou, Enhanced photocatalytic reduction of CO2 into alcohols on Z-scheme Ag/Ag3PO4/CeO2 driven by visible light, Mater. Lett. 232 (2018) 36–39.
[139] Y.G. Kim, W.K. Jo, Efficient decontamination of textile industry wastewater using a photochemically stable n-n type CdSe/Ag3PO4 heterostructured nanohybrid containing metallic Ag as a mediator, J. Hazard. Mater. 361 (2018) 64.
[140] T. Cai, Y. Liu, L. Wang, S. Zhang, Y. Zeng, J. Yuan, J. Ma, W. Dong, C. Liu, S. Luo, Silver phosphate-based Z-Scheme photocatalytic system with superior sunlight photocatalytic activities and anti-photocorrosion performance, Appl. Catal. B 208 (2017) 1–13.
[141] W. Zhang, G. Li, W. Wang, Y. Qin, T. An, X. Xiao, W. Choi, Enhanced photocatalytic mechanism of Ag 3 PO 4 nano-sheets using MS 2 (M = Mo, W)/rGO hybrids as co-catalysts for 4-nitrophenol degradation in water, Appl. Catal. B (2018).
[142] H. Anwer, J.W. Park, Synthesis and characterization of a heterojunction rGO/ZrO2/Ag3PO4 nanocomposite for degradation of organic contaminants, J. Hazard. Mater. 358 (2018) 416.
[143] N. Shao, Z. Hou, H. Zhu, J. Wang, C.P. François-Xavier, Novel 3D core-shell structured CQDs/Ag 3 PO 4 @Benzoxazine tetrapods for enhancement of visible-light photocatalytic activity and anti-photocorrosion, Appl. Catal. B (2018).
[144] R. Qu, W. Zhang, N. Liu, Q. Zhang, Y. Liu, X. Li, Y. Wei, L. Feng, Antioil Ag3PO4 nanoparticle/polydopamine/Al2O3 sandwich structure for complex wastewater treatment: dynamic catalysis under natural light, ACS Sustainable Chem. Eng. 6 (2018) 8019–8028.
[145] Q. Guo, H. Li, Q. Zhang, Y. Zhang, Fabrication characterization and mechanism of a novel Z-scheme Ag 3 PO 4/NG/polyimide composite photocatalyst for microcystin-LR degradation, Appl. Catal. B (2018).
[146] H.Y. Si, C.J. Mao, J.Y. Zhou, X.F. Rong, Q.X. Deng, S.L. Chen, J.J. Zhao, X.G. Sun, Y.M. Shen, W.J. Feng, Z-scheme Ag3PO4/graphdiyne/g-C3 N4 composites: enhanced photocatalytic O 2 generation benefiting from dual roles of graphdiyne, Carbon 132 (2018) 598–605.
[147] J. Pan, C. Chi, M. You, Z. Jiang, W. Zhao, M. Zhu, C. Song, Y. Zheng, C. Li, The three dimensional Z-scheme Ag3PO4/Ag/MoS2/TiO2 nano-heterojunction and its sunlight photocatalytic performance enhancement, Mater. Lett. 227 (2018) 205–208.
[148] P. Zhou, J. Yu, M. Jaroniec, All-solid-state Z-scheme photocatalytic systems, Adv. Mater. 26 (2014) 4920–4935.
[149] J. Ran, J. Zhang, J. Yu, M. Jaroniec, S.Z. Qiao, Earth-abundant cocatalysts for semiconductor-based photocatalytic water splitting, Chem. Soc. Rev. 43 (2014) 7787–7812.
[150] X. Li, H. Hu, L. Xu, C. Cui, D. Qian, S. Li, W. Zhu, P. Wang, P. Lin, J. Pan, Z-schematic water splitting by the synergistic effect of a type-II heterostructure and a highly efficient oxygen evolution catalyst, Appl. Surf. Sci. 441 (2018) 61–68.
[151] S. Nayak, K.M. Parida, Dynamics of charge-transfer behavior in a plasmon-induced quasi-type-II p–n/n–n dual heterojunction in Ag@Ag3PO4/g-C3N4/NiFe LDH nanocomposites for photocatalytic Cr(VI) reduction and phenol oxidation, ACS Omega 3 (2018) 7324–7343.
[152] W. Liu, J. Shen, X. Yang, Q. Liu, H. Tang, Dual Z-scheme g-C3N4/Ag3PO4/Ag2MoO4 ternary composite photocatalyst for solar oxygen evolution from water splitting, Appl. Surf. Sci. 456 (2018) 369–378.
[153] M.A. Rauf, M.A. Meetani, S. Hisaindee, An overview on the photocatalytic degradation of azo dyes in the presence of TiO2 doped with selective transition metals, Desalination 276 (2011) 13–27.
[154] H. Park, Y. Park, W. Kim, W. Choi, Surface modification of TiO2 photocatalyst for environmental applications, J. Photochem. Photobiol., C 15 (2013) 1–20.
[155] D.Y. Leung, X. Fu, C. Wang, M. Ni, M.K. Leung, X. Wang, X. Fu, Hydrogen production over titania-based photocatalysts, ChemSusChem 3 (2010) 681–694.
[156] Y. Hanifehpour, B. Soltania, A.R. Amani-Ghadim, B. Hedayati, B. Khomami, W.J. Sang, Synthesis and characterization of samarium-doped ZnS nanoparticles: A novel visible light responsive photocatalyst, Mater. Res. Bull. 76 (2016) 411–421.
[157] M.N. Huda, Y. Yan, M.M. Aljassim, The delocalized nature of holes in (Ga, N) cluster-doped ZnO, J. Phys. Condensed Matter Instit. Phys. J. 24 (2012) 415503.
[158] L. Song, Z. Chen, T. Li, S. Zhang, A novel Ni2+-doped Ag3PO4 photocatalyst with high photocatalytic activity and enhancement mechanism, Mater. Chem. Phys. (2016).
[159] W.D.S. Pereira, J.C. Sczancoski, Y.N.C. Calderon, V.R. Mastelaro, G. Botelho, T.R. Machado, E.R. Leite, E. Longo, Influence of Cu substitution on the structural ordering, photocatalytic activity and photoluminescence emission of $Ag_{3-2x}Cu_xPO_4$ powders, Appl. Surf. Sci. 440 (2018).
[160] S. Zhang, S. Zhang, L. Song, Super-high activity of Bi3+ doped Ag3PO4 and enhanced photocatalytic mechanism, Appl. Catal. B 152–153 (2014) 129–139.
[161] A.B. Trench, T.R. Machado, A.F. Gouveia, M. Assis, L.G. da Trindade, C. Santos, A. Perrin, C. Perrin, M. Oliva, J. Andrés, E. Longo, Connecting structural, optical, and electronic properties and photocatalytic activity of Ag3PO4: Mo complemented by DFT calculations, Appl. Catal. B 238 (2018) 198–211.
[162] Y.P. Xie, G.S. Wang, Visible light responsive porous lanthanum-doped Ag3PO4 photocatalyst with high photocatalytic water oxidation activity, J. Colloid Interface Sci. 430 (2014) 1.
[163] E. Ghazalian, N. Ghasemi, A.R. Amani-Ghadim, Enhanced visible light photocatalytic performance of Ag3PO4 through doping by different trivalent Lanthanide

cations, Mater. Res. Bull. 88 (2017) 23–32.
[164] E. Ghazalian, N. Ghasemi, A.R. Amani-Ghadim, Effect of gadollunium doping on visible light photocatalytic performance of Ag3PO4: evaluation of activity in degradation of an anthraquinone dye and mechanism study, J. Mol. Catal. A: Chem. 426 (2017) 257–270.
[165] H. Yu, H. Kang, Z. Jiao, G. Lü, Y. Bi, Tunable photocatalytic selectivity and stability of Ba-doped Ag3PO4 hollow nanosheets, Chin. J. Catal. 36 (2015) 1587–1595.
[166] J. Zhang, Y. Wu, M. Xing, S.A.K. Leghari, S. Sajjad, Development of modified N doped TiO2 photocatalyst with metals, nonmetals and metal oxides, Energy Environ. Sci. 3 (2010) 715–726.
[167] G. Liu, L. Wang, H.G. Yang, H.M. Cheng, G.Q. Lu, Titania-based photocatalysts—crystal growth, doping and heterostructuring, J. Mater. Chem. 20 (2010) 831–843.
[168] S. Liu, J. Yu, B. Cheng, M. Jaroniec, Fluorinated semiconductor photocatalysts: tunable synthesis and unique properties, Adv. Colloid Interface Sci. 173 (2012) 35–53.
[169] S. Li, S. Shi, G. Huang, Y. Xiong, S. Liu, Synergetic tuning charge dynamics and potentials of Ag3PO4 photocatalysts with boosting activity and stability by facile in-situ fluorination, Appl. Surf. Sci. 455 (2018) 1137–1149.
[170] W.J. Jo, J.W. Jang, K.J. Kong, H.J. Kang, J.Y. Kim, H. Jun, K.P. Parmar, J.S. Lee, Phosphate doping into monoclinic BiVO4 for enhanced photoelectrochemical water oxidation activity, Cheminform 43 (2012) 3201–3205.
[171] H. Huang, X. Li, J. Wang, F. Dong, P.K. Chu, T. Zhang, Y. Zhang, Anionic group self-doping as a promising strategy: band-gap engineering and multi-functional applications of high-performance CO32-Doped Bi2O2CO3, ACS Catal. 5 (2015) 150603114219008.
[172] W. Cao, Z. Gui, L. Chen, X. Zhu, Z. Qi, Facile synthesis of sulfate-doped Ag 3 PO 4 with enhanced visible light photocatalystic activity, Appl. Catal. B 200 (2017) 681–689.
[173] J. Luo, Y. Luo, Q. Li, J. Yao, G. Duan, X. Liu, Synthesis of doughnut-like carbonate-doped Ag 3 PO 4 with enhanced visible light photocatalytic activity, Colloids Surf., A (2017).
[174] Y. Xie, S. Luo, H. Huang, Z. Huang, Y. Liu, M. Fang, X. Wu, X. Min, Construction of an Ag 3 PO 4 morphological homojunction for enhanced photocatalytic performance and mechanism investigation, Colloids Surf., A 546 (2018) 99–106.
[175] Y. Bi, H. Hu, S. Ouyang, Z. Jiao, G. Lu, J. Ye, Selective growth of Ag3PO4 submicro-cubes on Ag nanowires to fabricate necklace-like heterostructures for photocatalytic applications, J. Mater. Chem. 22 (2012) 14847–14850.
[176] Q. Zhu, X. Hu, M.S. Stanislaus, N. Zhang, R. Xiao, N. Liu, Y. Yang, A novel P/Ag/Ag 2 O/Ag 3 PO 4/TiO 2 composite film for water purification and antibacterial application under solar light irradiation, Sci. Total Environ. 577 (2016) 236–244.
[177] M.N. Subramaniam, P.S. Goh, W.J. Lau, B.C. Ng, A.F. Ismail, AT-POME colour removal through photocatalytic submerged filtration using antifouling PVDF-TNT nanocomposite membrane, Sep. Purif. Technol. 191 (2017).
[178] J. Pacheco, M. Prairie, L. Evans, L. Yellowhorse, Engineering-scale experiments of solar photocatalytic oxidation of trichloroethylene, Proceedings of the 25th Intersociety Energy Conversion Engineering Conference, 1990, pp. 141–145.
[179] J.V. Anderson, H. Link, M. Bohn, B. Gupta, Development of solar detoxification technology in the USA - an introduction, Solar Energy Mater. 24 (1991) 538–549.
[180] P.A.S.S. Marques, M.F. Rosa, F. Mendes, M.C. Pereira, J. Blanco, S. Malato, Wastewater detoxification of organic and inorganic toxic compounds with solar collectors, Desalination 108 (1997) 213–220.
[181] R. Goslich, R. Dillert, D. Bahnemann, Solar water treatment: principles and reactors, Water Sci. Technol. 35 (1997) 137–148.
[182] D. Curcó, S. Malato, J. Blanco, J. Giménez, P. Marco, Photocatalytic degradation of phenol: comparison between pilot-plant-scale and laboratory results, Sol. Energy 56 (1996) 387–400.
[183] C. Minero, E. Pelizzetti, S. Malato, J. Blanco, Large solar plant photocatalytic water decontamination: degradation of atrazine, Sol. Energy 56 (1996) 411–419.
[184] S. Malato, J. Blanco, C. Richter, D. Curcó, J. Gimenez, Low-concentrating CPC collectors for photocatalytic water detoxification: comparison with a medium concentrating solar collector, Water Sci. Technol. 35 (1997) 157–164.
[185] C. Minero, E. Pelizzetti, S. Malato, J. Blanco, Large solar plant photocatalytic water decontamination: degradation of pentachlorophenol, Chemosphere 26 (1993) 2103–2119.
[186] S.M. Rodriguez, C. Richter, J.B. Galvez, M. Vincent, Photocatalytic degradation of industrial residual waters, Sol. Energy 56 (1996) 401–410.
[187] S. Malato, J. Blanco, A. Vidal, C. Richter, Photocatalysis with solar energy at a pilot-plant scale: an overview, Appl. Catal. B 37 (2002) 1–15.
[188] S.M. RodríGuez, J.B. Gálvez, M.I.M. Rubio, P.F. Ibáñez, D.A. Padilla, M.C. Pereira, J.F. Mendes, J.C.D. Oliveira, Engineering of solar photocatalytic collectors, Sol. Energy 77 (2004) 513–524.
[189] D. Spasiano, R. Marotta, S. Malato, P. Fernandez-Ibañez, I.D. Somma, Solar photocatalysis: Materials, reactors, some commercial, and pre-industrialized applications. A comprehensive approach, Appl. Catal. B Environ. 170–171 (2015) 90–123.
[190] C. Heinemann, X. Xing, K.D. Warzecha, P. Ritterskamp, H. Görner, M. Demuth, An asymmetric induction principle and biomimetics with photons via electron transfer, Pure Appl. Chem. 70 (1998) 2167–2176.
[191] R. Dillert, A.E. Cassano, R. Goslich, D. Bahnemann, Large scale studies in solar catalytic wastewater treatment, Catal. Today 54 (1999) 267–282.
[192] T.F.C.V. Silva, M.E.F. Silva, A.C. Cunha-Queda, A. Fonseca, I. Saraiva, A.R.B. Rui, V.J.P. Vilar, Sanitary landfill leachate treatment using combined solar photo-Fenton and biological oxidation processes at pre-industrial scale, Chem. Eng. J. 228 (2013) 850–866.
[193] W. Gernjak, M.I. Maldonado, S. Malato, J. Cáceres, T. Krutzler, A. Glaser, R. Bauer, Pilot-plant treatment of olive mill wastewater (OMW) by solar TiO photocatalysis and solar photo-Fenton, Sol. Energy 77 (2004) 567–572.
[194] M. Kositzi, I. Poulios, S. Malato, J. Caceres, A. Campos, Solar photocatalytic treatment of synthetic municipal wastewater, Water Res. 38 (2004) 1147–1154.
[195] W. Gernjak, T. Krutzler, A. Glaser, S. Malato, J. Caceres, R. Bauer, A.R. Fernándezalba, Photo-Fenton treatment of water containing natural phenolic pollutants, Chemosphere 50 (2003) 71–78.
[196] I. Oller, W. Gernjak, M.I. Maldonado, L.A. Pérez-Estrada, J.A. Sánchez-Pérez, S. Malato, Solar photocatalytic degradation of some hazardous water-soluble pesticides at pilot-plant scale, J. Hazard. Mater. 138 (2006) 507–517.
[197] S.M. Rodríguez, J.B. Gálvez, M.I. Rubio, P.F. Ibáñez, W. Gernjak, I.O. Alberola, Treatment of chlorinated solvents by TiO2 photocatalysis and photo-Fenton: influence of operating conditions in a solar pilot plant, Chemosphere 58 (2005) 391–398.
[198] S. Malato, J. Blanco, M.I. Maldonado, I. Oller, W. Gernjak, L. Pérez-Estrada, Coupling solar photo-Fenton and biotreatment at industrial scale: main results of a demonstration plant, J. Hazard. Mater. 146 (2007) 440–446.
[199] V. Sarria, S. Kenfack, O. Guillod, C. Pulgarin, An innovative coupled solar-biological system at field pilot scale for the treatment of biorecalcitrant pollutants, J. Photochem. Photobiol., A 159 (2003) 89–99.
[200] Y.K. Abdel-Maksoud, E. Imam, A.R. Ramadan, Sand supported TiO 2 photocatalyst in a tray photo-reactor for the removal of emerging contaminants in wastewater, Catal. Today (2017).
[201] O.M. Alfano, D. Bahnemann, A.E. Cassano, R. Dillert, R. Goslich, Photocatalysis in water environments using artificial and solar light, Catal. Today 58 (2000) 199–230.
[202] K.C. Lee, K.H. Choo, Optimization of flocculation conditions for the separation of TiO 2 particles in coagulation-photocatalysis hybrid water treatment, Chem. Eng. Process. Process Intensif. 78 (2014) 11–16.
[203] N. Güy, K. Atacan, E. Karaca, M. Özacar, Role of Ag3PO4 and Fe3O4 on the photocatalytic performance of magnetic Ag3PO4/ZnO/Fe3O4 nanocomposite under visible light irradiation, Sol. Energy 166 (2018).
[204] Y. Zan, M. Zhai, Y. Ni, Construction and improved photocatalytic performance of Fe 3 O 4 @resorcinol–formaldehyde-resins/Ag3PO4/Ag/AgBr magnetic multi-component catalyst, J. Mater. Sci.: Mater. Electron. (2018) 1–10.
[205] E. Abroshan, S. Farhadi, A. Zabardasti, Novel magnetically separable Ag3PO4/MnFe2O4 nanocomposite and its high photocatalytic degradation performance for organic dyes under solar-light irradiation, Sol. Energy Mater. Sol. Cells 178 (2018) 154–163.
[206] S. Huang, Y. Xu, T. Zhou, M. Xie, Y. Ma, Q. Liu, L. Jing, H. Xu, H. Li, Constructing magnetic catalysts with in-situ solid-liquid interfacial photo-Fenton-like reaction over Ag3PO4@NiFe2O4 composites, Appl. Catal. B 225 (2018) 40–50.
[207] I.M. Arabatzis, T. Stergiopoulos, M.C. Bernard, D. Labou, S.G. Neophytides, P. Falaras, Silver-modified titanium dioxide thin films for efficient photodegradation of methyl orange, Appl. Catal. B 42 (2003) 187–201.
[208] R.L. Pozzo, M.A. Baltanás, A.E. Cassano, Towards a precise assessment of the performance of supported photocatalysts for water detoxification processes, Catal. Today 54 (1999) 143–157.
[209] H. Yu, Z. Jiao, H. Hu, G. Lu, J. Ye, Y. Bi, Fabrication of Ag3PO4 –PAN composite nanofibers for photocatalytic applications, CrystEngComm 15 (2013) 4802–4805.
[210] H. Yu, Q. Dong, Z. Jiao, W. Teng, J. Ma, G. Lu, Y. Bi, Ion exchange synthesis of PAN/Ag3PO4 core–shell nanofibers with enhanced photocatalytic properties, J. Mater. Chem. A 2 (2014) 1668–1671.
[211] X.Q. Wu, J.S. Shen, F. Zhao, Z.D. Shao, L.B. Zhong, Y.M. Zheng, Flexible electrospun MWCNTs/Ag3PO4/PAN ternary composite fiber membranes with enhanced photocatalytic activity and stability under visible-light irradiation, J. Mater. Sci. (2018) 1–13.
[212] F. Almomani, R. Bhosale, A. Kumar, M. Khraisheh, Potential use of solar photocatalytic oxidation in removing emerging pharmaceuticals from wastewater: a pilot plant study, Sol. Energy 172 (2018) 128–140.
[213] X.Y. Xu, C. Chu, H. Fu, X.D. Du, P. Wang, W. Zheng, C.C. Wang, Light-responsive UiO-66-NH2/Ag3PO4 MOF-nanoparticle composites for the capture and release of sulfamethoxazole, Chem. Eng. J. 350 (2018) 436–444.